Atmospheric
Chemistry
and Physics
Discussions

The Secondary Formation of Organosulfates under the Interactions between Biogenic Emissions and Anthropogenic Pollutants in Summer of Beijing

Yujue Wang,[1] Min Hu,[*,1,5] Song Guo,[1] Yuchen Wang,[3] Jing Zheng,[1] Yudong Yang,[1] Wenfei Zhu,[6] Rongzhi Tang,[1] Xiao Li,[1] Ying Liu,[1,5] Michael Le Breton,[2] Zhuofei Du,[1] Dongjie Shang,[1] Yusheng Wu,[1] Zhijun Wu,[1] Yu Song,[1] Shengrong Lou,[6] Mattias Hallquist,[2] and Jianzhen Yu [*,3,4]

[1]State Key Joint Laboratory of Environmental Simulation and Pollution Control, College of Environmental Sciences and Engineering, Peking University, Beijing 100871, China

[2]Department of Chemistry and Molecular Biology, University of Gothenburg, Gothenburg, Sweden

[3]Environmental Science Programs, Hong Kong University of Science & Technology, Hong Kong, China

[4]Department of Chemistry, Hong Kong University of Science & Technology, Hong Kong, China

[5]Beijing Innovation Center for Engineering Sciences and Advanced Technology, Peking University, Beijing 100871, China

[6]Shanghai Academy of Environmental Sciences, Shanghai 200233, China

Correspondence to: Min Hu (minhu@pku.edu.cn); Jianzhen Yu (jian.yu@ust.hk)

Abstract. Organosulfates (OSs), with ambiguous formation mechanisms, are a potential source of "missing secondary organic aerosol (SOA)" in current atmospheric models. In this study, we analyzed the characterization and formation of OSs and nitrooxy OSs (NOSs) under the influence of biogenic emissions and anthropogenic pollutants (e.g. NO_x, SO_4^{2-}) in summer of Beijing. The ultrahigh-resolution mass spectrometer equipped with electrospray ionization source was applied to examine the overall molecular composition of S-containing organics. The number and intensities of S-containing organics, majority of which could be assigned as OSs and NOSs, increased significantly during pollution episodes, which indicated their importance for SOA accumulation. To further investigate the distribution and formation of OSs and NOSs, the high performance liquid chromatography coupled to mass spectrometer was then employed to quantify ten representative OSs and three NOS species. The total concentrations of quantified OSs and NOSs were 41.42 and 13.75 ng/m^3, respectively. Glycolic acid sulfate was the most abundant species among all the quantified species, followed by monoterpene NOSs ($C_{10}H_{16}NO_7S^-$). The total concentration of three isoprene OSs was 14.77 ng/m^3 and the isoprene OSs formed via HO_2 channel was higher than those formed via NO/NO_2 channel. The OS concentration coincided with the increase of acidic sulfate aerosols, aerosol

Atmospheric
Chemistry
and Physics
Discussions

Open Access

EGU

27 acidity and liquid water content, indicating the acid-catalyzed aqueous-phase formation of OSs in the presence of acidic

28 sulfate aerosols. When sulfate dominated the accumulation of secondary inorganic aerosols (SIAs) (SO_4^{2-}/SIAs> 0.5), OS

29 formation would be obviously promoted as the increasing of acidic sulfate aerosols, aerosol LWC and acidity (pH< 2.8).

30 Otherwise, the acid-catalyzed OS formation would be limited by lower aerosol acidity when nitrate dominated the SIA

31 accumulation. The nighttime enhancement of monoterpene NOSs suggested their formation via nighttime NO_3-initiated

32 oxidation of monoterpene under high-NO_x conditions. However, isoprene NOSs are supposed to form via acid-catalyzed

33 chemistry or reactive uptake of oxidation products of isoprene. This study provides direct observational evidence and

34 highlights the secondary formation of OSs and NOSs, via the interaction between biogenic precursors and anthropogenic

35 pollutants (NO_x, SO_2 and SO_4^{2-}). The results imply that future reduction in anthropogenic emissions can help to reduce the

36 biogenic SOA burden in Beijing or other areas impacted by both biogenic emissions and anthropogenic pollutants.

37 **1   Introduction**

38   Secondary organic aerosols (SOA), formed by atmospheric oxidation of volatile organic compounds (VOCs), accounts

39 for a large fraction of organic aerosols (OA) on the global scale   (Jimenez et al., 2009; Guo et al., 2014). However, current

40 models usually underestimate (Kroll and Seinfeld, 2008; Hallquist et al., 2009) or predict the SOA concentration with large

41 uncertainties (Jimenez et al., 2009; Kiehl, 2007; Shrivastava et al., 2017) in ambient atmosphere. Thus, it is important to

42 elucidate potential missing groups of compounds or formation mechanisms. Organosulfates (OSs), commonly formed via the

43 interaction between VOC precursors and acidic sulfate seed particles, could be a potential source of "missing SOA" in

44 current atmospheric models (Surratt et al., 2010). OSs have been observed in various ambient atmospheres, including urban,

45 rural, suburban, forest as well as remote environments (Lin et al., 2012; Meade et al., 2016; Stone et al., 2012; Riva et al.,

46 2015; Brüggemann et al., 2017), which could represent 0.02-30% of OA (Hawkins et al., 2010; Stone et al., 2012; Frossard

47 et al., 2011; Tolocka and Turpin, 2012; Surratt et al., 2008; Liao et al., 2015).

48   Many chamber experiments studied try to reveal the precursors and formation mechanisms of OSs (Surratt et al., 2010;

49 Surratt et al., 2008; Liggio and Li, 2006; Chan et al., 2011; Shalamzari et al., 2014; Shalamzari et al., 2016; Zhang et al.,

Atmospheric
Chemistry
and Physics
Discussions

Open Access

EGU

50   2012), which remain unclear. Various biogenic VOCs (BVOCs) precursors have been reported, including isoprene (Hatch et

51   al., 2011; Surratt et al., 2010), monoterpenes (Surratt et al., 2008), sesquiterpenes (Chan et al., 2011), pinonaldehyde (Liggio

52   and Li, 2006), unsaturated aldehydes (Shalamzari et al., 2014; Shalamzari et al., 2016) and 2-methyl-3-buten-2-ol (Zhang et

53   al., 2012). OSs originating from isoprene are some of the most studied compounds and could be among the most abundant

54   OA in some areas (Liao et al., 2015; Chan et al., 2010; Surratt et al., 2010; Lin et al., 2013a; Worton et al., 2013). Isoprene

55   OSs usually form through ring-opening epoxide chemistry catalyzed by acidic sulfate aerosols (Worton et al., 2013; Froyd et

56   al., 2010; Paulot et al., 2009). OSs were also proposed to form by reactive uptake of VOCs or their oxidation products that

57   involves the sulfate radicals (Nozière et al., 2010; Schindelka et al., 2013). The alcohol sulfate esterification was also a

58   source of OSs, while it was predicted to be kinetically insignificant under ambient tropospheric conditions after lab bulk

59   phase experiments (Minerath et al., 2008). Nitrooxy organosulfates (NOSs) were observed to form via the nighttime

60   NO_3-initiated oxidation of VOC precursors (e.g. monoterpene), followed by alcohol sulfate esterification (Iinuma et al., 2007;

61   Surratt et al., 2008). Organic nitrate ($R-ONO_2$) could also act as precursors to OSs through the nucleophilic substitution of

62   nitrate by sulfate (Hu et al., 2011; Darer et al., 2011).

63   Both aerosol acidity and liquid water content (LWC) are key variables influencing the OS formation processes. OS

64   formation could only happen in the presence of sulfate aerosols, enhanced by increased aerosol acidity, through

65   acid-catalyzed reactive uptake and multiphase reactions of oxidation products (Riva et al., 2016b; Surratt et al., 2010; Lal et

66   al., 2012). Previous studies also demonstrated the importance of aqueous-phase or heterogeneous reactions for OS formation

67   (Lal et al., 2012; McNeill et al., 2012; McNeill, 2015). On one hand, the increased LWC would decrease the aerosol viscosity,

68   which favors the exchange of organics or other gas molecules into the particles, mass diffusion of reactants and

69   heterogeneous chemical reactions within the particles (Vaden et al., 2011; Booth et al., 2014; Renbaum-Wolff et al., 2013),

70   and thereby enhance the OS formation. On the other hand, more LWC would lead to increased pH due to dilution. For

71   example, Riva et al. (2016) and Duporte et al. (2016) found that the OS formation decreased with higher RH, which was

72   attributed to the increased pH as a result of higher LWC (Duporte et al., 2016; Riva et al., 2016b).

73   To get a comprehensive understanding of the characteristics and formation of OSs in the ambient atmosphere, it is

74   desirable to simultaneously identify and quantify particulate OSs on the molecular level. Soft ionization techniques coupled

Atmospheric
Chemistry
and Physics
Discussions

75 with ultrahigh-resolution mass spectrometer (UHRMS) have been widely applied to identify various and numerous organics,

76 including OS species, in ambient aerosols or chamber studies (Lin et al., 2012; Blair et al., 2017; Tao et al., 2014; Wang et al.,

77 2016). UHRMS is a powerful analytical tool in gaining an overall characterization of OSs, however, the quantification

78 capability is limited without pre-separation. High performance liquid chromatography coupled to mass spectrometer

79 (HPLC-MS) is suitable for the separation and quantification of different OS compounds. However, one noted limitation is a

80 lack of commercially available authentic standards. As a result, surrogate standards are often used for quantification (He et

81 al., 2014; Riva et al., 2015; Zhang et al., 2012), which adds uncertainty to the concentrations (Wang et al., 2017d). Recently,

82 a few research groups quantified some OS species using synthetic authentic standards (e.g. hydroxyacetone sulfate, glycolic

83 acid sulfate, lactic acid sulfate, methyltetrol sulfate, aromatic OSs, α/β-pinene OS，Limonene OS and Limonaketone OS)

84 (Hettiyadura et al., 2017; Hettiyadura et al., 2015; Olson et al., 2011; Wang et al., 2017d; Ma et al., 2014; Budisulistiorini et

85 al., 2015; Staudt et al., 2014), which was very important for understanding the variation and formation of OSs in ambient

86 aerosols.

87   Missing knowledge of formation mechanisms, the complexities of ambient aerosol composition and oxidation condition,

88 and the lack of commercially available standards all hinder us from understanding the formation and fate of OSs in ambient

89 atmosphere. In this study, particulate OSs were comprehensively characterized to provide direct observational evidence to

90 shed insights into OS formation under the influence of both biogenic and anthropogenic sources in summertime Beijing.

91 Orbitrap MS coupled with soft ionization source was used to identify the overall molecular composition of S-containing

92 organics. HPLC-MS was then applied to quantify some representative OSs and NOS species using newly synthesized

93 authentic standards and surrogate standards. The characterization and formation pathways of OSs and NOSs were elaborated.

94 Using OSs as examples, this work illustrates the anthropogenic-biogenic interactions and SOA formation in areas with

95 abundant anthropogenic pollutants and natural emissions.

Atmospheric
Chemistry
and Physics
Discussions

2   Methods

2.1 Sample collection

This study was a part of the bilateral Sweden-China framework research program on 'Photochemical smog in China: formation, transformation, impact and abatement strategies', focusing on the SOA formation under the influence of anthropogenic pollutants (Hallquist et al., 2016). An intensive field campaign was conducted at Changping (40.14° N, 116.11° E), a regional site 38 km northeast of the Beijing urban area, China. The campaign was conducted from May 15 to June 23, 2016, when the site was influenced by high biogenic emissions from vegetation in the nearby mountains and anthropogenic pollutants from the nearby villages and Beijing urban areas (Tang et al., 2017). During May 17- June 5, the average concentrations of isoprene, monoterpene, benzene, toluene and NO_x were 297, 83, 441, 619 pptv and 22.7 ppb, respectively.

Ambient aerosols were collected from May 16 to June 5. $PM_{2.5}$ (particles with aerodynamic diameter less than 2.5 μm) samples were collected on prebaked quartz fiber filters (Whatman Inc.) and Teflon filters (Whatman Inc.) using a high-volume sampler (TH-1000C, Tianhong, China) and a 4-channel sampler (TH-16A, Tianhong, China). The sampling flow rate was 1.05 m^3/min and 16.7 L/min, respectively. The daytime samples were collected from 8:30 to 17:30 and nighttime ones from 18:00 to 8:00 the next morning. Field blank samples were collected by placing filters in the samplers with the pump off for 30 min. The period May 20 - June 3 will be discussed in this study.

2.2 Orbitrap MS analysis

An Exactive Plus-Orbitrap MS (Thermo Scientific Inc., Bremen, Germany) equipped with a heated electrospray ionization (ESI) source was used to identify the overall molecular composition of OSs. Details of the extraction and data analysis have been described in Wang et al. (2017c). Briefly, a portion of filter was extracted with ultrapure water in an ultrasonic bath for 40 min and the extracts were filtered with 0.45 μm pore size PTFE syringe filter (Gelman Sciences). The filter portion size was adjusted to yield ~ 200 μg OC in each extract, in order to decrease the variation of ion suppression arising from varying coexisting $PM_{2.5}$ components. The extract sample was then loaded onto a solid phase extraction (SPE) cartridge (DSC-18, Sigma-Aldrich, USA) to remove inorganic ions and low molecular weight (MW) organic acids (Lin et al.,

Atmospheric
Chemistry
and Physics
Discussions

120   2010), followed by elution with methanol. The methanol eluate was dried under a gentle stream of N_2 and re-dissolved in

121   acetonitrile/water (1:1) solvent for Orbitrap MS analysis.

122   The Orbitrap MS was operated in negative mode (ESI-). The mass calibration was conducted using a standard mixture

123   of N-butylamine, caffeine, MAFA, sodium dodecyl sulfate, sodium taurocholate and Ultramark 1621, with the scan range set

124   to be 90-900 m/z. The Orbitrap MS had a mass resolution of 140,000 at m/z =200. Each sample was analyzed for three times

125   with at least 100 full-scan spectra acquired in each analysis. The recorded mass spectra were processed and exported using

126   the Xcalibur software (V2.2, Thermo Scientific). Peaks with a signal-to-noise ratio ≥10 were exported. All the

127   mathematically possible formulas for each ion were calculated with a mass tolerance of 2 ppm. Each exported molecular

128   formula was allowed containing certain elements and limited by several conservative rules (Wang et al., 2017c). The

129   background spectra were obtained by analyzing the corresponding field blank sample following the same procedure. Peaks

130   were eliminated from the list if their intensities were lower than ten times of those in the blank sample.

131   **2.3 Quantification of OSs and NOSs using HPLC-MS**

132   An aliquot of 25 cm^2 was removed from each filter sample and extracted in ultrasonic bath three times using 3, 2 and 1

133   mL methanol consecutively, each time for 30 min. The extracts were then filtered through a 0.25 μm polytetrafluoroethylene

134   (PTFE) syringe filter (Pall Life Sciences), combined, evaporated to dryness under a gentle stream of high-purity nitrogen and

135   re-dissolved in 50 μL methanol/water (1:1) containing 1 ppm D_{17}-octyl sulfate as internal standard. The solution was

136   centrifuged and the supernatant was used for analysis, using Agilent 1260 LC system (Palo Alto, CA) coupled to QTRAP

137   4500 (AB Sciex, Toronto, Ontario, Canada) mass spectrometer. The LC/MS was equipped with an ESI source operated in

138   negative mode. The optimized MS conditions and details of the method have been described in our previous study (Wang et

139   al., 2017d). Chromatographic separation was performed on an Acquity UPLC HSS T3 column (2.1 mm×100 mm, 1.8 μm

140   particle size; Waters, USA) with a guard column (HSS T3, 1.8 μm). The mobile eluents were (A) water containing 0.1%

141   acetic acid (v/v) and (B) methanol (v/v) containing 0.1% acetic acid at a flow rate of 0.19 mL/min. The gradient elution was

142   set as follows: the composition started with 1% B for 2.7 min; increased to 54% B within 12.5 min and held for 1.0 min; then

Atmospheric
Chemistry
and Physics
Discussions

Open Access

EGU

143 increased to 90% B within 7.5 min and held for 0.2 min; and finally decreased to 1% B within 1.8 min and held for 17.3 min

144 until the column was equilibrated. The column temperature was kept at 45 ^{o}C and the injection volume was 5.0 μL.

145 The quantified OSs and NOS species are listed in Table 1. The monoterpene NOSs ($C_{10}H_{16}NO_7S^-$ and $C_9H_{14}NO_8S^-$)

146 were quantified using the [M-H]$^-$ ions in the extracted ion chromatogram (EIC) and other species were quantified in

147 multiple-reaction monitoring (MRM) mode. OSs and NOSs were quantified using authentic standards or surrogates with

148 similar molecular structures (Table 1). Lactic acid sulfate (LAS) and glycolic acid sulfate (GAS) were prepared according to

149 Olson et al. (2011) (Olson et al., 2011). Four monoterpene derived OSs were synthesized according to Wang et al. (2017)

150 (Wang et al., 2017d).

151 **2.4 Other online and offline measurements**

152 A high resolution time-of-flight aerosol mass spectrometer (AMS) was employed to measure the chemical composition

153 of PM_1. The operation procedures and data analysis have been described in Zheng et al. (2017) (Zheng et al., 2017). VOCs

154 were measured by a proton-transfer-reaction mass spectrometer (PTR-MS). Meteorological parameters, including relative

155 humidity (RH), temperature, wind direction and wind speed (WS) were continuously monitored during the campaign.

156 Organic carbon (OC) was analyzed using thermal/optical carbon analyzer (Sunset Laboratory). The organic matter (OM)

157 concentration was calculated by multiplying OC by 1.6 (Turpin and Lim, 2001). Water soluble inorganic ions and low MW

158 organic acids were quantified by an ion chromatograph (IC, DIONEX, ICS2500/ICS2000) following procedures described in

159 Guo et al. (2010). After performing quality assurance/quality control for IC measurements, the data (ions, pH, LWC) derived

160 from IC measurements in the daytime samples of May 26 and 29 were excluded in the following analysis. Gaseous NH_3 was

161 measured using a NH_3 analyzer (G2103, Picarro, California, USA) (Huo et al., 2015). Aqueous phase [H^+] and LWC were

162 then calculated with the ISORROPIA-II thermodynamic model. ISORROPIA-II was operated in forward mode, assuming

163 the particles are "metastable" (Hennigan et al., 2015; Weber et al., 2016; Guo et al., 2015). The input parameters included:

164 ambient RH, temperature, particle phase inorganic species (SO_4^{2-}, NO_3^-, Cl^-, NH_4^+, K^+, Na^+, Ca^{2+}, Ma^{2+}) and gaseous NH_3.

Atmospheric
Chemistry
and Physics
Discussions

3   Results and discussion

3.1 Overall molecular characterization of S-containing organics

All the formulas identified by Orbitrap MS in ESI negative mode were classified into four major categories based on their elemental compositions, including CHO, CHON, CHOS and CHONS. As an example, CHONS refers to compounds that contain C, H, O, N and S elements in the formula. Other compound categories are defined analogously. The percent of different compound categories in terms of number and intensity are shown in Fig. S1 and Fig. 1, in which 'others' refer to the compounds excluded from the above major compound categories. During pollution episodes, the percent of S-containing compounds (CHOS and CHONS) increased obviously in both number percent (Fig. S1) and intensity percent (Fig. 1). The OC content in each sample for Orbitrap MS analysis was kept roughly constant to minimize variation arising from matrix ion suppression. Taking the nighttime sample of May 24 (0524N) as an example of clean days and the nighttime sample of May 30 (0530N) as an example of polluted days, the mass spectra of different compound categories in each sample are shown and compared in Fig. 1 (a) and (b). The increase in S-containing organics indicated their more important contribution to SOA when the pollution accumulated. What's more, the S-containing compounds contributed more to the higher MW formulas than CHO (O_1-O_{10}) or CHON (O_1-O_{11}) compounds (Fig. 1), due to the existence of more O (CHOS: O_1-O_{12}, CHONS: O_1-O_{14}) atoms and heteroatoms (S, N) in the molecules. They may play more important roles in the increase of SOA mass concentrations during pollution episodes.

The CHOS formulas with O/S$\geq$ 4 allow the possible assignment of a sulfate group in the molecules (i.e., OSs) (Lin et al., 2012). Among all the identified CHOS formulas, 60%-99% (93% on average) and 66-100% (96% on average) of them could be assigned as OSs in terms of number and intensity percent. Analogously, the CHONS formulas with O/(S+N)$\geq$ 7 could likely be NOSs formulas, which account for 22-78% (53% on average) by number and 18-94% (61% on average) by intensity of all the identified CHONS formulas. As OSs and NOSs were assigned based on the molecular formulas alone, we could not completely exclude the possibility of CHOS being hydroxysulfonates and CHONS being nitro-OSs due to the lack of MS/MS analysis. According to previous study, the presences of organosulfonate or nitro-OSs were usually limited compared to those of OSs or nitrooxy-OSs (Lin et al., 2012), thus they were not taken into consideration in this study. A total

189   of 351 OSs and 181 NOSs formulas were identified among all the samples during the campaign. The temporal variation of

190   the total number and intensity of OSs and NOSs are shown in Fig. S1. During pollution episodes (nighttime of May 27 - the

191   nighttime of May 28, nighttime of May 29 - the nighttime of May 30), the total number and intensity of OSs formulas

192   increased (Fig. S1). The total number of NOSs also showed similar increase trend during pollution episodes, while the total

193   intensity of NOSs showed nighttime enhancement during the whole observation period (Fig. S1). Previous studies suggested

194   that some NOS species could form via NO_3-initiated oxidation under high-NO_x conditions at night (Surratt et al., 2008;

195   Iinuma et al., 2007; Gomez-Gonzalez et al., 2008), which will be further discussed in the following sections.

196   Some of the more abundant OSs and NOS peaks identified in the samples on the clean day (05/24N) or during pollution

197   episodes (05/30D, 05/30N) are listed in Table S1. For example, deprotonated molecules $C_9H_{15}SO_7^-$, $C_{10}H_{17}SO_7^-$ and

198    $C_9H_{17}SO_6^-$ were observed among the highest OS peaks in samples during pollution episodes (Table S1). These compounds

199   could be derived from the oxidation of alkanes or diesel fuel based on previous chamber studies (Riva et al., 2016b; Blair et

200   al., 2017). OS compounds derived from anthropogenic VOC precursors were widely observed in ambient aerosols (Table

201   S1), while they were not quantified due to the lack of standards in this paper. They will be further investigated in our future

202   studies. Other OSs molecules (e.g. $C_9H_{15}SO_6^-$, $C_{10}H_{17}SO_5^-$) could be formed via the oxidation of monoterpene (Surratt et al.,

203   2008). For NOSs, molecules $C_{10}H_{16}NO_7S^-$, $C_{10}H_{16}NO_9S^-$ and $C_{10}H_{16}NO_{10}S^-$ were among the highest peaks (Table S1). They

204   could form via the nighttime NO_3-initiated oxidation of monoterpenes (Surratt et al., 2008). These are just some examples

205   with relatively higher relative intensity (RI). The RI may not accurately represent their relative concentration levels in each

206   sample, as the MS responses of different OSs are also influenced by different carbon chain structures (Wang et al., 2017d).

207   The OS species of low MW and short carbon chain structures (with less than 6 carbon atoms in the molecule) are little

208   retained on the SPE cartridges due to their highly water-soluble and more hydrophilic properties (Gomez-Gonzalez et al.,

209   2008; Lin et al., 2012; Lin et al., 2010). As such, they were largely absent among the OS formulas detected by Orbitrap MS

210   in this work. Hydroxyacetone sulfate ($C_3H_5O_5S^-$) was detected by Orbitrap MS only in several samples with relatively higher

211   concentrations. Hydroxycarboxylic acid sulfate ($C_2H_3O_6S^-$, $C_3H_5O_6S^-$) or isoprene OSs ($C_4H_7O_7S^-$, $C_5H_7O_7S^-$, $C_5H_{11}O_7S^-$) are

212   also sufficiently hydrophilic that little of them would be in the SPE eluate fraction, which was subjected for Orbitrap MS

213   analysis. This explains why these highly water-soluble OS species with lower MW are absent in Fig. 1. Though these OS

214 species were not detected by Orbitrap MS, some of them were quantified with high concentrations in the ambient aerosols in

215 the LC/MS analysis (Table 1), as the sample aliquots for the LC/MS analysis did not involve SPE treatment.

3.2 Abundance of identified OSs and NOSs in ambient aerosols

217   To further investigate the abundance and formation pathways of OSs and NOSs in ambient aerosols, some

218 representative species were then quantified by HPLC-MS using anthentic standards when available or surrogate standards. A

219 total of ten OSs and three NOS species were quantified in this study and their concentrations are listed in Table 1. The

220 molecules with the same molecular formula were treated as one species (e.g., monoterpene NOSs with [M-H]$^-$ at m/z 294

221 were treated as one NOS species). The total concentrations of quantified OSs were 41.42 ng/m^3, accounting for 0.3% of OM,

222 with a maximum contribution of 0.7% on the night of May 30. The total concentrations of quantified NOSs were 13.75

223 ng/m^3, corresponding to 0.1% of OM, with a maximum contribution of 0.4% on the night of May 23.

224   The relative contribution of each species to the total OSs or NOSs is shown in Fig. 2. GAS was the most abundant

225 species among all the quantified species. The concentrations of GAS were 3.86-58.16 ng/m^3, with an average of 19.50 ng/m^3.

226 The concentrations were higher than those observed in Mexico (4.1- 7.0 ng/m^3), California (3.3- 5.4 ng/m^3), Pakistan (11.3

227 ng/m^3) or Centreville (14 ng/m^3) (Olson et al., 2011; Hettiyadura et al., 2015). The GAS concentration level at Beijing was

228 comparable to those reported in summertime Alabama (20.6-26.2 ng/m^3), a location characterized by high biogenic

229 emissions and affected by anthropogenic pollutants (Hettiyadura et al., 2017; Rattanavaraha et al., 2016). The concentrations

230 of LAS were 0.74-11.94 ng/m^3, with an average of 4.39 ng/m^3. The LAS concentrations were also higher than those

231 observed in Mexico (1.2-1.8 ng/m^3), California (0.6-0.8 ng/m^3) or Pakistan (3.8 ng/m^3), while lower than those observed in

232 Centreville (19 ng/m^3) or Alabama (16.5 ng/m^3) (Olson et al., 2011; Hettiyadura et al., 2015; Hettiyadura et al., 2017).

233 Carboxylic acids mainly form via aqueous-phase oxidation in cloud or particle water, including both biogenic and

234 anthropogenic sources (Charbouillot et al., 2012; Chebbi and Carlier, 1996). The relatively higher level of

235 hydroxycarboxylic acid sulfate could be attributed to the favorable interaction between sulfate aerosols and carboxylic acids

236 or other precursors in summertime Beijing, while the precursors and mechanisms remain unclear. Strong inter-correlations

237 were found among GAS, LAS and hydroxyacetone sulfate (HAS) (Table S2), indicating their potentially similar precursors

Atmospheric
Chemistry
and Physics
Discussions

238 or formation pathways. They also showed strong correlations with isoprene OSs (Table S2), suggesting isoprene or its

239 oxidized products as potential precursors of GAS, LAS and HAS. It is suggested that both hydroxyacetone and carboxylic

240 acids could be produced from the oxidation of isoprene (Fu et al., 2008; Carlton et al., 2009). GAS, LAS and HAS have been

241 reported to form via isoprene oxidation in the presence of acidic sulfate (Riva et al., 2016a; Surratt et al., 2008). GAS was

242 also observed to form via sulfate induced oxidation of methyl vinyl ketone (MVK), oxidation product of isoprene

243 (Schindelka et al., 2013).

244   The total concentration of isoprene OSs ($C_4H_7O_7S^-$, $C_5H_7O_7S^-$ and $C_5H_{11}O_7S^-$) was 14.77 ng/m^3, contributing to 36 % of

245 the total quantified OSs in this study. The isoprene OSs were lower than those observed in southeastern US, with substantial

246 isoprene emissions and impacted by anthropogenic pollutants, in which authentic standards were employed to quantify the

247 isoprene OSs (Rattanavaraha et al., 2016). We used lactic acid sulfate as a surrogate standard to quantify isoprene OSs due to

248 their similar structures and retention times (Table 1). The isoprene concentration in southeastern US (1.9 ppb) (Xu et al.,

249 2015) is much higher than that observed during our campaign (297 pptv). Moreover, the OM-coating particle structures

250 observed in Beijing could reduce the reactive uptake of isoprene oxidation products (Li et al., 2016; Zhang et al., 2018),

251 which may be another possible reason for lower isoprene OSs in this study. The concentrations were comparable to those

252 observed in suburban area of mid-Atlantic or Belgium and higher than those observed at the background site of Pearl River

253 Delta (PRD) region (Meade et al., 2016; Gómez-González et al., 2012; He et al., 2014), in which glycolic sulfate ester,

254 ethanesulfonic acid or camphor sulfonic acid were employed as surrogate standards. The isoprene OSs formed via HO$_2$

255 channel ($C_5H_{11}O_7S^-$) were observed to be higher than that formed via NO/NO$_2$ channel ($C_4H_7O_7S^-$) (Table 1) (Worton et al.,

256 2013). Isoprene had higher mixing ratio during the daytime (Fig. S2 (b)), when OH radicals dominated the atmospheric

257 oxidation capacity. Furthermore, the yield of isoprene oxidation via HO$_2$ channel is proposed to be higher than that via

258 NO/NO$_2$ channel (Worton et al., 2013). The concentration of $C_5H_7O_7S^-$ was comparable to that of $C_5H_{11}O_7S^-$ (Table 1).

259 $C_5H_7O_7S^-$ was suggested to be formed via isoprene oxidation and related to $C_5H_{11}O_7S^-$ (Surratt et al., 2008), while the

260 formation mechanism remains unclear. The concentration of isoprene NOSs ($C_5H_{10}NO_9S^-$) was lower than that of individual

261 isoprene OSs. Strong inter-correlations were observed between isoprene OSs and NOSs (Table S2), suggesting their similar

262 formation pathways.

263   The average concentration of monoterpene OSs (α-pinene OSs, β-pinene OSs, limonene OSs and limonaketone OSs)

264   was 0.57 ng/m^3, lower than those observed in mid-Atlantic (Meade et al., 2016) or the Pearl River Delta in southern China

265   where more abundant emissions of BVOC precursors are expected (Wang et al., 2017d; He et al., 2014). The contribution of

266   monoterpene OSs was much lower than that of isoprene OSs or other OSs (Fig. 2, Table 1), as the mixing ratio of

267   monoterpene (83 pptv) was lower than that of isoprene (297 pptv) during the campaign. Furthermore, the reactivity of

268   monoterpene with OH radical is lower than that of isoprene (Carlton et al., 2009; Paulot et al., 2009; Atkinson et al., 2006).

269   Different from isoprene OSs, the four monoterpene OS species didn't show strong correlations with each other (Table S2),

270   which may suggest their different oxidation mechanisms. While the contribution of monoterpene OSs were low, the

271   monoterpene NOSs ($C_{10}H_{16}NO_7S^-$) were the second most abundant species among all the quantified species (Table 1),

272   especially in the nighttime samples. The concentration of monoterpene NOSs ($C_{10}H_{16}NO_7S^-$) was much higher than those

273   observed in mid-Atlantic or Belgium (Meade et al., 2016; Gómez-González et al., 2012), while lower than that observed in

274   Pearl River Delta, South China (He et al., 2014). $C_{10}H_{16}NO_7S^-$ was also identified to be among the highest peaks in the mass

275   spectra recorded by Orbitrap MS (Fig. 1 (b)), with a RI of 83% in the sample of 05/30N (Table S1). The monoterpene NOSs

276   could be formed via nighttime NO_3-initiated oxidation under high-NO_x conditions (Surratt et al., 2008; Iinuma et al., 2007;

277   Gomez-Gonzalez et al., 2008). During the observation, both monoterpenes and NO_x showed higher mixing ratios at night

278   (Fig. S2 (a), (d)), favorable for the NO_3-initiated formation of NOSs.

279   **3.3 OS formation via acid-catalyzed aqueous-phase chemistry**

280   The time series of the total OS concentrations quantified by HPLC-MS are shown in Fig. 3, along with the

281   meteorological conditions, SO_2, aerosol LWC, acidity, $PM_{2.5}$ and the major chemical components. Most OS species showed

282   similar trends to the total OSs (Fig. S3), except for α-pinene OSs and β-pinene OSs, observed at very low concentrations.

283   During the campaign, particles were generally acidic with a pH range of 2.0- 3.7, favorable for the OS formation (Fig. 3).

284   The OS concentrations generally followed similar trend with that of sulfate aerosols (Fig. 3), suggesting the OS formation in

285   the presence of acidic sulfate aerosols.

286   During the observation period, three pollution episodes (episodes I, II, III) were identified based on the $PM_{2.5}$

Atmospheric
Chemistry
and Physics
Discussions

287   concentrations, which are marked by gray shadow in Fig. 3. The most significant increase trend of OSs was observed during

288   pollution episode III (nighttime of May 29 - the nighttime of May 30). During this episode, the accumulation of secondary

289   inorganic aerosols (SIAs), referring to sulfate, nitrate and ammonium in this study, was dominated by sulfate. SIAs,

290   especially sulfate and nitrate salts, represent the most important components driving the particle hygroscopicity (Wu et al.,

291   2018; Xue et al., 2014), thus the aerosol LWC increased with SIAs (Fig. 3). The increase of aerosol acidity, indicated by

292   aqueous phase $[H^+]$, was also observed during this episode (Fig. 3). OSs increased to the highest level (129.15 ng/m^3) during

293   the campaign under the condition of high sulfate aerosols, high aerosol acidity and LWC (Fig. 3), suggesting the

294   acid-catalyzed aqueous-phase formation of OSs in the presence of acidic sulfate aerosols. Moreover, the higher aerosol LWC

295   encountered during these periods would favor the uptake of gas-phase reactants into particle phase, due to the decrease of

296   viscosity and increase of diffusivity within the particles (Shiraiwa et al., 2011). During pollution episode II (nighttime of

297   May 27 - the nighttime of May 28), the OS concentration level was lower than that during episode III. It is noted that the

298   increase of sulfate, aerosol LWC and acidity were also less than that during episode III, indicating less aqueous-phase

299   formation of OSs. During this episode, the increase of SIAs was attributed to both sulfate and nitrate, the two with

300   comparable contribution to the total SIAs. Different from episodes II and III, the SIAs accumulation was dominated by

301   nitrate during episode I (May 21- 23). OS and sulfate aerosols stayed at medium concentration level, lower than those during

302   the other two episodes. During the daytime of May 21, aerosol acidity increased due to the elevated relative contribution of

303   sulfate than that of nitrate, thus the OS concentration also increased. During the daytime of May 23, higher aerosol LWC

304   was observed as the rapid increasing of nitrate, while the aerosol acidity was lower due to the less contribution of sulfate

305   compared with nitrate. Thus, the increase of OS concentration was not very obvious. The OS formation may be limited by

306   the aerosol acidity, indicating the importance of acid-catalyzed chemistry. This episode ended with the rain elimination event

307   on the afternoon of May 23. The OSs were at low concentrations from May 24 to the daytime of May 27, when sulfate, SO$_2$,

308   aerosol acidity and LWC were noticeably lower than the other periods, restraining the OS formation.

309   The three pollution episodes were characterized by different inorganic aerosol composition and aerosol properties (e.g.

310   acidity, LWC), resulting in different levels of OS formation. The concentrations and relative contribution of sulfate, aerosol

311   acidity and LWC are important factors influencing OS formation. The OS concentrations generally increased with the

Atmospheric
Chemistry
and Physics
Discussions
Open Access
EGU

312 increasing of sulfate, aerosol acidity and LWC (Fig. 3), suggesting more active OS formation via acid-catalyzed

313 aqueous-phase reactions in the presence of sulfate. These influencing factors were interrelated. Both sulfate and nitrate are

314 important hygroscopic components (Chan and Chan, 2005; Wu et al., 2018; Xue et al., 2014), favoring the water uptake of

315 aerosols and thus increasing LWC. The increasing of aerosol LWC with SIAs was observed (Fig. 3). A previous study also

316 suggested that at a given RH, aerosol LWC was nearly linearly related to the sum of nitrate and sulfate mass concentrations

317 (Guo et al., 2016). The variation of SIA composition and LWC would then influence the aerosol acidity (Liu et al., 2017;

318 Guo et al., 2016). In this study, higher aerosol acidity was observed with elevated contribution of sulfate among SIAs (Fig.

319 3). This is in accord with a previous study suggesting that particle pH was generally below 2 when aerosol anionic

320 composition was dominated by sulfate ($NO_3^-/2SO_4^{2-}$ mole ratio >1) (Guo et al., 2016).

321   To further elucidate the major factors influencing OS formation and their interrelations with SIA compositions, the

322 distribution of OS concentrations as a function of SO_4^{2-}/SIAs ratios and other related factors are plotted in Fig. 4. The aerosol

323 LWC generally increased with the increasing of the SIA mass concentrations, while the aerosol acidity was also influenced

324 by the relative contribution of SO_4^{2-} and NO_3^- to SIAs (Fig. 4 (b)). When the SIAs were dominated by SO_4^{2-} (SO_4^{2-}/SIAs>

325 0.5), the aerosol acidity increased obviously as a function of SO_4^{2-}/SIAs ratios and the pH values were generally below 2.8

326 (Fig. 4 (b)). The high aerosol acidity was favorable for OS formation and OS concentration also increased as a function of

327 sulfate mass concentration and fraction (Fig. 4 (a)). The pollution episode III (Fig. 3) was the typical case for this condition.

328 When the SIAs were dominated by nitrate (SO_4^{2-}/SIAs< 0.5), high LWC may occur due to the high concentrations of

329 hygroscopic SIAs, while the aerosol acidity was relatively lower due to the lower sulfate fraction than that of nitrate (Fig. 4

330 (b)). The increase trend of OSs as a function of sulfate or SO_4^{2-}/SIAs ratios was not as obvious as the sulfate-dominant

331 condition (SO_4^{2-}/SIAs> 0.5), as the OS formation may be limited by lower aerosol acidity. The daytime of May 23 during

332 pollution episode I (Fig. 3) was the typical case for this atmospheric condition. Overall, the OS formation would obviously

333 be promoted via acid-catalyzed aqueous-phase reactions, when the SIAs accumulation was dominated by sulfate (SO_4^{2-}/SIAs>

334 0.5).

Atmospheric
Chemistry
and Physics
Discussions

3.4 Monoterpene NOS formation via the nighttime NO_3 oxidation

335

336   A recent study suggested that nearly all the BVOCs could be oxidized overnight, dominated by reactions via NO_3

337   oxidation, at a NO_x/BVOCs ratio higher than 1.4 (Edwards et al., 2017). When we roughly estimated the BVOCs

338   concentration to be the sum of isoprene, MVK+MACR, and monoterpenes, the NO_x/BVOCs ratios were higher than 10 at

339   night (Fig. S3). This indicated the dominant nighttime BVOCs loss via NO_3-initiated oxidation in summer of Beijing. The

340   oxidation of BVOCs was found to be controlled by NO_3 oxidation rather than O_3 oxidation during the campaign, which

341   contributed to a total of 90% of BVOCs reactivity at night (Wang et al., 2018). Nighttime enhancement of monoterpene

342   NOSs was clearly observed under high-NO_x conditions (Fig. 5). The nighttime concentrations of $C_{10}H_{16}NO_7S^-$ and

343     $C_9H_{14}NO_8S^-$ were respectively 2.3-32.4 (10.8 on average) and 1.9-20.7 (6.8 on average) times of the daytime concentrations.

344   Higher mixing ratios of monoterpenes were observed at night (Fig. S2), when the high NO_x concentrations (Fig. 5) favored

345   the formation of monoterpene NOSs via NO_3-initiated oxidation of monoterpenes. The nighttime formation of monoterpene

346   NOSs was also observed in previous studies (Surratt et al., 2008; Iinuma et al., 2007; Gomez-Gonzalez et al., 2008). High

347   correlation between N_2O_5 and NO_2 or NO_3 radical production were observed (Wang et al., 2018), so the NO_2 concentration

348   was employed to investigate NO_3 oxidation during the campaign in this study. Higher concentrations of monoterpene NOSs

349   ($C_{10}H_{16}NO_7S^-$) were found with elevated NO_2 level at night (Fig. 6), indicating the plausibility of more NOS formation via

350   NO_3-initiated oxidation. When NO_2 increased to higher than 20 ppb, the NOS concentration did not further increase

351   obviously with NO_2, which suggested that NO_2 was in surplus and not the limiting factor for NOS formation any more.

352   The lower concentrations of monoterpene NOSs during the daytime could be attributed to the much lower production,

353   as the monoterpene, NO_x and NO_x/BVOCs ratios were much lower than those at night (Fig. S2). What's more, monoterpene

354   NOSs, also as organic nitrate (R-ONO_2) compounds, may go through decomposition via photolysis or OH oxidation during

355   the daytime (He et al., 2011; Suarez-Bertoa et al., 2012). Organic nitrates have been estimated to have a short lifetime of

356   several hours (Lee et al., 2016). Elevation in concentrations of monoterpene NOSs were also observed with the increasing of

357   NO_2 during daytime, but the concentrations were much lower and the increase was less prominent than that during the

358   nighttime (Fig. 6). The highest daytime concentration of $C_{10}H_{16}NO_7S^-$ was recorded on May 23 (10.59 ng/m^3), followed by

Atmospheric
Chemistry
and Physics
Discussions

Open Access

EGU

359   the daytime of May 31 (8.03 ng/m^3). The NO_2 concentrations were in the range of 20-25 ppb and 10-15 ppb during the

360   daytime of May 23 and 31, respectively. It is noted that the $J(O^1D)$ values during the daytime of May 23 and 31 were much

361   lower than other daytime periods (Fig. 5), indicating the possibility of less decomposition of monoterpene NOSs. Previous

362   studies also reported that the organic nitrate have much shorter lifetimes than the corresponding OSs, thus it is possible that

363   organic nitrates derived from monoterpene would undergo nucleophilic attack by sulfate and form monoterpene OSs or

364   NOSs (He et al., 2014; Darer et al., 2011; Hu et al., 2011). Monoterpene NOSs could also undergo hydrolysis and form

365   monoterpene OSs (Darer et al., 2011; Hu et al., 2011). These may be other potential pathways for the loss of monoterpene

366   NOSs and production of monoterpene OSs. These potential formation pathways of monoterpene OSs were different from the

367   formation pathways via acid-catalyzed aqueous-phase reactions. This could be another explanation for the different temporal

368   variations of some monoterpene OSs (Fig. S3) from other OSs.

3.5 Formation pathways of isoprene OSs and NOSs

370   Different from the day-night variation trend of monoterpene NOSs, isoprene NOSs ($C_5H_{11}NO_9S^-$) displayed similar

371   temporal variation to isoprene OSs and the total OSs (Fig. 7). The isoprene NOSs are supposed to form via similar pathways

372   as isoprene OSs, rather than the nighttime NO_3-initiated oxidation pathway as that of monoterpene NOSs. The strong

373   correlation between isoprene OSs and NOSs also indicated their similar formation pathways (Table S2). The oxidation of

374   isoprene could form isoprene epoxydiols (IEPOX), hydroxymethyl-methyl-lactone (HMML) or methacrolein (MACR) and

375   methacrylic acid epoxide (MAE) (Paulot et al., 2009; Lin et al., 2013b; Worton et al., 2013; Nguyen et al., 2015). The

376   isoprene OSs could then be formed through ring-opening epoxide chemistry, which was shown to be a kinetically feasible

377   pathway (Minerath and Elrod, 2009; Worton et al., 2013). Isoprene OSs were also proposed to form by reactive uptake and

378   oxidation of MVK or MACR (oxidation products of isoprene) initiated by the sulfate radicals (Nozière et al., 2010;

379   Schindelka et al., 2013). Isoprene NOSs generally increased with the increasing of isoprene oxidation products

380   (MVK+MACR) and acidic sulfate aerosols (Figs. 3 and 7). It indicates isoprene NOSs are supposed to form via

381   acid-catalyzed reactions or reactive uptake of oxidation products of isoprene by sulfate, rather than NO_3-initiated oxidation

382   pathways. In the formation pathways of isoprene OSs or NOSs, epoxide first form carbocation intermediates through

383   acid-catalyzed hydrolysis reactions, and then sulfate ions serve as nucleophiles in the subsequent fast step forming OSs or

384   NOSs (Minerath and Elrod, 2009). The presence of high levels of sulfate may effectively facilitate the ring-opening reaction

385   of epoxide or reactive uptake of oxidation products and subsequent OSs or NOS formation (Surratt et al., 2010). The

386   proposed formation mechanisms of isoprene NOSs are needed to be further investigated and validated through laboratory

387   studies.

388   Although the isoprene NOS formation was not via the NO_3-initiated oxidation pathways, the NO_3 radical could be

389   involved in the formation pathways and influence the yield of isoprene NOSs. Considering the different atmospheric

390   conditions during the daytime and nighttime, we analyzed the variation of daytime and nighttime isoprene NOSs separately

391   (Fig. 8). Generally, higher concentrations of isoprene NOSs were found with elevated NO_2 or MVK+MACR concentration

392   levels. During daytime, the correlation of isoprene NOSs with NO_2 was higher than that with MVK+MACR (Fig. 8). When

393   MVK+MACR was higher than 0.7 ppb, the NOS concentrations did not increase with MVK+MACR any more. It was likely

394   that the biogenic VOCs precursors were in surplus under this condition and the formation of isoprene NOSs may be limited

395   by the lower daytime NO_2 concentration, sulfate aerosols or other factors. During daytime, the MVK+MACR concentrations

396   were generally higher and NO_x was lower (Fig. S2), thus the NO_2 level may limit the daytime formation of isoprene NOSs.

397   During nighttime, strong correlation between isoprene NOSs and MVK+MACR was observed, while the increase trend of

398   isoprene NOSs as a function of NO_2 level was not so obvious and their correlation was lower (Fig. 8). During nighttime, the

399   NO_x concentrations were generally higher and MVK+MACR concentrations were lower (Fig. S2), thus the concentrations of

400   isoprene oxidation products (e.g. MVK+MACR) may be the limiting factor for the nighttime formation of isoprene NOSs.

401   The threshold (e.g. NO_x/isoprene ratio, NO_x/isoprene oxidation products ratio) that makes the transition from NO_x-limited to

402   isoprene-limited (or isoprene oxidation products) still need further investigation through laboratory studies.

403   **4   Conclusions**

404   An intensive field campaign was conducted to investigate the characterization and formation of OSs and NOSs in

405   summer of Beijing, under the influence of abundant biogenic emissions and anthropogenic pollutants (e.g. NO_x, SO_2 and

Atmospheric
Chemistry
and Physics
Discussions

406   SO_4^{2-}). The overall molecular characterization of S-containing organics (CHOS, CHONS) was made through ESI-Orbitrap

407   MS data. More than 90% of the CHOS formulas could be assigned as OSs and more than half of the CHONS formulas could

408   be assigned as NOSs, based on the molecular formulas. The number and intensity of OSs and NOSs increased significantly

409   during pollution episodes, which indicated they might play important roles for the SOA accumulation.

410   To further investigate the distribution and formation pathways of OSs and NOSs in complex ambient atmosphere, some

411   representative species were quantified using HPLC-MS, including ten OSs and three NOS species. The total concentrations

412   of quantified OSs and NOSs were 41.42 and 13.75 ng/m^3, respectively, accounting for 0.3% and 0.1% of organic matter.

413   Glycolic acid sulfate was the most abundant species (19.50 ng/m^3) among all the quantified OS species. The strong

414   correlations between GAS, LAS, HAS and isoprene OSs indicated their potential formation pathways via isoprene oxidation

415   in the presence of acidic sulfate aerosols. The concentration of isoprene OSs was 14.77 ng/m^3 and the isoprene OSs formed

416   via HO_2 channel was higher than that via NO/NO_2 channel. The contribution of monoterpene OSs was much smaller than

417   other OSs, while the monoterpene NOSs ($C_{10}H_{16}NO_7S^-$) were observed at high concentration (11.99 ng/m^3), especially in

418   nighttime samples.

419   OS concentration generally increased with the increase of acidic sulfate aerosols, aerosol acidity and LWC, indicating

420   the acid-catalyzed aqueous-phase formation of OSs in the presence of acidic sulfate aerosols as an effective formation

421   pathway. The sulfate concentration, SIA composition, aerosol acidity, and LWC are important factors influencing the OS

422   formation. When sulfate dominated the SIAs accumulation (SO_4^{2-}/SIAs> 0.5), the aerosol acidity would increase obviously

423   as a function of SO_4^{2-}/SIAs ratios and the pH values were generally below 2.8. Thus, the OS formation would be obviously

424   promoted as the increasing of acidic sulfate aerosols, aerosol acidity and LWC. When the SIAs accumulation were

425   dominated by nitrate (SO_4^{2-}/SIAs< 0.5), high aerosol LWC may occur, while the OS formation via acid-catalyzed reactions

426   may be limited by relatively lower aerosol acidity.

427   The NO_3-initiated oxidation dominated the nighttime BVOCs loss in summertime Beijing, with the NO_x/BVOCs ratios

428   higher than 10 at night. Significant nighttime enhancement of monoterpene NOSs was observed, indicating the formation via

429   NO_3-initiated oxidation of monoterpene under high-NO_x conditions. Higher concentrations of monoterpene NOSs were

430   found with elevated NO_2 level at night and NO_2 ceased to be a limiting factor for NOS formation when higher than 20 ppb.

18

Atmospheric
Chemistry
and Physics
Discussions

431 The lower daytime concentrations of monoterpene NOSs could be attributed to the lower production and the decomposition

432 during daytime. Different from the monoterpene NOS formation via NO_3-initiated oxidation, isoprene NOSs and OSs are

433 supposed to form via acid-catalyzed chemistry or reactive uptake of the oxidation products of isoprene, which is needed to

434 be further investigated through laboratory studies. The daytime NO_2 concentration could be a limiting factor for isoprene

435 NOS formation, while the nighttime formation was limited by isoprene or its oxidation products. The proposed formation

436 mechanisms of isoprene NOSs as well as the limiting factors still need further investigation in laboratory studies.

437   This study highlights the formation of OSs and NOSs via the interaction between biogenic VOC precursors and

438 anthropogenic pollutants (NO_x, SO_2 and SO_4^{2-}) in summer of Beijing. Our study reveals the accumulation of OSs with the

439 increase of acidic sulfate aerosols and the nighttime enhancement of monoterpene NOSs under high-NO_x conditions. The

440 acidic sulfate aerosols and high nighttime NO_x or N_2O_5 concentrations were observed in Beijing in our observation and also

441 other studies (Liu et al., 2017; Wang et al., 2017b; Wang et al., 2017a), which provide favorable conditions for the formation

442 of OSs and NOSs. The results imply the importance of reducing anthropogenic emissions, especially NO_x and SO_2, to reduce

443 the biogenic SOA burden in Beijing, and also in areas with abundant biogenic emissions and anthropogenic pollutants.

444 Moreover, the OSs or NOSs could be treated as key SOA species when exploring the biogenic-anthropogenic interactions as

445 well as organic-inorganic reactions.

446

447 *Data availability.* The dataset is available upon request by contacting Min Hu (minhu@pku.edu.cn).

448

449 **The Supplement related to this article is available online**

450

451 *Competing interests.* The authors declare that they have no conflict of interest.

452

Atmospheric
Chemistry
and Physics
Discussions

References

459   Atkinson, R., Baulch, D. L., Cox, R. A., Crowley, J. N., Hampson, R. F., Hynes, R. G., Jenkin, M. E., Rossi, M. J., Troe, J.,
460   and Subcommittee, I.: Evaluated kinetic and photochemical data for atmospheric chemistry: Volume II - gas phase reactions
461   of organic species, Atmos. Chem. Phys., 6, 3625-4055, 10.5194/acp-6-3625-2006, 2006.

462   Blair, S. L., MacMillan, A. C., Drozd, G. T., Goldstein, A. H., Chu, R. K., Pasa-Tolic, L., Shaw, J. B., Tolic, N., Lin, P.,
463   Laskin, J., Laskin, A., and Nizkorodov, S. A.: Molecular Characterization of Organosulfur Compounds in Biodiesel and
464   Diesel Fuel Secondary Organic Aerosol, Environ. Sci. Technol., 51, 119-127, 10.1021/acs.est.6b03304, 2017.

465   Booth, A. M., Murphy, B., Riipinen, I., Percival, C. J., and Topping, D. O.: Connecting bulk viscosity measurements to
466   kinetic limitations on attaining equilibrium for a model aerosol composition, Environ. Sci. Technol., 48, 9298-9305,
467   10.1021/es501705c, 2014.

468   Brüggemann, M., Poulain, L., Held, A., Stelzer, T., Zuth, C., Richters, S., Mutzel, A., van Pinxteren, D., Iinuma, Y.,
469   Katkevica, S., Rabe, R., Herrmann, H., and Hoffmann, T.: Real-time detection of highly oxidized organosulfates and BSOA
470   marker compounds during the F-BEACh 2014 field study, Atmos. Chem. Phys., 17, 1453-1469, 10.5194/acp-17-1453-2017,
471   2017.

472   Budisulistiorini, S. H., Li, X., Bairai, S. T., Renfro, J., Liu, Y., Liu, Y. J., McKinney, K. A., Martin, S. T., McNeill, V. F., Pye,
473   H. O. T., Nenes, A., Neff, M. E., Stone, E. A., Mueller, S., Knote, C., Shaw, S. L., Zhang, Z., Gold, A., and Surratt, J. D.:
474   Examining the effects of anthropogenic emissions on isoprene-derived secondary organic aerosol formation during the 2013
475   Southern Oxidant and Aerosol Study (SOAS) at the Look Rock, Tennessee ground site, Atmos. Chem. Phys., 15, 8871-8888,
476   10.5194/acp-15-8871-2015, 2015.

477   Carlton, A. G., Wiedinmyer, C., and Kroll, J. H.: A review of Secondary Organic Aerosol (SOA) formation from isoprene,
478   Atmos. Chem. Phys., 9, 4987-5005, 10.5194/acp-9-4987-2009, 2009.

479   Chan, M. N., and Chan, C. K.: Mass transfer effects in hygroscopic measurements of aerosol particles, Atmos. Chem. Phys.,
480   5, 2703-2712, 10.5194/acp-5-2703-2005, 2005.

481   Chan, M. N., Surratt, J. D., Claeys, M., Edgerton, E. S., Tanner, R. L., Shaw, S. L., Zheng, M., Knipping, E. M., Eddingsaas,
482   N. C., Wennberg, P. O., and Seinfeld, J. H.: Characterization and quantification of isoprene-derived epoxydiols in ambient
483   aerosol in the southeastern United States, Environ. Sci. Technol., 44, 4590-4596, 10.1021/es100596b, 2010.

484   Chan, M. N., Surratt, J. D., Chan, A. W. H., Schilling, K., Offenberg, J. H., Lewandowski, M., Edney, E. O., Kleindienst, T.
485   E., Jaoui, M., Edgerton, E. S., Tanner, R. L., Shaw, S. L., Zheng, M., Knipping, E. M., and Seinfeld, J. H.: Influence of
486   aerosol acidity on the chemical composition of secondary organic aerosol from β-caryophyllene, Atmos. Chem. Phys., 11,
487   1735-1751, 10.5194/acp-11-1735-2011, 2011.

488   Charbouillot, T., Gorini, S., Voyard, G., Parazols, M., Brigante, M., Deguillaume, L., Delort, A.-M., and Mailhot, G.:

489   Mechanism of carboxylic acid photooxidation in atmospheric aqueous phase: Formation, fate and reactivity, Atmos. Environ.,
490   56, 1-8, 10.1016/j.atmosenv.2012.03.079, 2012.

491   Chebbi, A., and Carlier, P.: Carboxylic acids in the troposphere, occurrence, sources, and sinks: A review, Atmos. Environ.,
492   30, 4233-4249, 10.1016/1352-2310(96)00102-1, 1996.

493   Darer, A. I., Cole-Filipiak, N. C., O'Connor, A. E., and Elrod, M. J.: Formation and stability of atmospherically relevant
494   isoprene-derived organosulfates and organonitrates, Environ. Sci. Technol., 45, 1895-1902, 10.1021/es103797z, 2011.

495   Duporte, G., Flaud, P. M., Geneste, E., Augagneur, S., Pangui, E., Lamkaddam, H., Gratien, A., Doussin, J. F., Budzinski, H.,
496   Villenave, E., and Perraudin, E.: Experimental Study of the Formation of Organosulfates from α-Pinene Oxidation. Part I:
497   Product Identification, Formation Mechanisms and Effect of Relative Humidity, The journal of physical chemistry. A, 120,
498   7909-7923, 10.1021/acs.jpca.6b08504, 2016.

499   Edwards, P. M., Aikin, K. C., Dube, W. P., Fry, J. L., Gilman, J. B., de Gouw, J. A., Graus, M. G., Hanisco, T. F., Holloway,
500   J., Huber, G., Kaiser, J., Keutsch, F. N., Lerner, B. M., Neuman, J. A., Parrish, D. D., Peischl, J., Pollack, I. B., Ravishankara,
501   A. R., Roberts, J. M., Ryerson, T. B., Trainer, M., Veres, P. R., Wolfe, G. M., Warneke, C., and Brown, S. S.: Transition from
502   high- to low-NOx control of night-time oxidation in the southeastern US, Nature Geosci., 10, 490-495, 10.1038/NGEO2976,
503   2017.

504   Frossard, A. A., Shaw, P. M., Russell, L. M., Kroll, J. H., Canagaratna, M. R., Worsnop, D. R., Quinn, P. K., and Bates, T. S.:
505   Springtime Arctic haze contributions of submicron organic particles from European and Asian combustion sources, J.
506   Geophys. Res., [Atmos.], 116, Artn D0520510.1029/2010jd015178, 2011.

507   Froyd, K. D., Murphy, S. M., Murphy, D. M., de Gouw, J. A., Eddingsaas, N. C., and Wennberg, P. O.: Contribution of
508   isoprene-derived organosulfates to free tropospheric aerosol mass, Proc. Natl. Acad. Sci. USA, 107, 21360-21365,
509   10.1073/pnas.1012561107, 2010.

510   Fu, T.-M., Jacob, D. J., Wittrock, F., Burrows, J. P., Vrekoussis, M., and Henze, D. K.: Global budgets of atmospheric
511   glyoxal and methylglyoxal, and implications for formation of secondary organic aerosols, J. Geophys. Res., 113,
512   10.1029/2007jd009505, 2008.

513   Gómez-González, Y., Wang, W., Vermeylen, R., Chi, X., Neirynck, J., Janssens, I. A., Maenhaut, W., and Claeys, M.:
514   Chemical characterisation of atmospheric aerosols during a 2007 summer field campaign at Brasschaat, Belgium: sources
515   and source processes of biogenic secondary organic aerosol, Atmos. Chem. Phys., 12, 125-138, 10.5194/acp-12-125-2012,
516   2012.

517   Gomez-Gonzalez, Y., Surratt, J. D., Cuyckens, F., Szmigielski, R., Vermeylen, R., Jaoui, M., Lewandowski, M., Offenberg, J.
518   H., Kleindienst, T. E., Edney, E. O., Blockhuys, F., Van Alsenoy, C., Maenhaut, W., and Claeys, M.: Characterization of
519   organosulfates from the photooxidation of isoprene and unsaturated fatty acids in ambient aerosol using liquid
520   chromatography/(-) electrospray ionization mass spectrometry, J. Mass Spectrom., 43, 371-382, 10.1002/jms.1329, 2008.

521   Guo, H., Xu, L., Bougiatioti, A., Cerully, K. M., Capps, S. L., Hite, J. R., Carlton, A. G., Lee, S. H., Bergin, M. H., Ng, N. L.,
522   Nenes, A., and Weber, R. J.: Fine-particle water and pH in the southeastern United States, Atmos. Chem. Phys., 15,
523   5211-5228, 10.5194/acp-15-5211-2015, 2015.

524   Guo, H., Sullivan, A. P., Campuzano-Jost, P., Schroder, J. C., Lopez-Hilfiker, F. D., Dibb, J. E., Jimenez, J. L., Thornton, J.
525   A., Brown, S. S., Nenes, A., and Weber, R. J.: Particle pH and the Partitioning of Nitric Acid during Winter in the

526   Northeastern United States, J. Geophys. Res., [Atmos.], 121, 10355-10376, 10.1002/2016JD025311, 2016.

527   Guo, S., Hu, M., Wang, Z. B., Slanina, J., and Zhao, Y. L.: Size-resolved aerosol water-soluble ionic compositions in the

528   summer of Beijing: implication of regional secondary formation, Atmos. Chem. Phys., 10, 947-959,

529   10.5194/acp-10-947-2010, 2010.

530   Guo, S., Hu, M., Zamora, M. L., Peng, J., Shang, D., Zheng, J., Du, Z., Wu, Z., Shao, M., Zeng, L., Molina, M. J., and Zhang,

531   R.: Elucidating severe urban haze formation in China, Proc. Natl. Acad. Sci. USA, 111, 17373-17378,

532   10.1073/pnas.1419604111, 2014.

533   Hallquist, M., Wenger, J. C., Baltensperger, U., Rudich, Y., Simpson, D., Claeys, M., Dommen, J., Donahue, N. M., George,

534   C., Goldstein, A. H., Hamilton, J. F., Herrmann, H., Hoffmann, T., Iinuma, Y., Jang, M., Jenkin, M. E., Jimenez, J. L.,

535   Kiendler-Scharr, A., Maenhaut, W., McFiggans, G., Mentel, T. F., Monod, A., Prevot, A. S. H., Seinfeld, J. H., Surratt, J. D.,

536   Szmigielski, R., and Wildt, J.: The formation, properties and impact of secondary organic aerosol: current and emerging

537   issues, Atmos. Chem. Phys., 9, 5155-5236, 10.5194/acp-9-5155-2009, 2009.

538   Hallquist, M., Munthe, J., Hu, M., Wang, T., Chan, C. K., Gao, J., Boman, J., Guo, S., Hallquist, A. M., Mellqvist, J.,

539   Moldanova, J., Pathak, R. K., Pettersson, J. B. C., Pleijel, H., Simpson, D., and Thynell, M.: Photochemical smog in China:

540   scientific challenges and implications for air-quality policies, Natl. Sci. Rev., 3, 401-403, 10.1093/nsr/nww080, 2016.

541   Hatch, L. E., Creamean, J. M., Ault, A. P., Surratt, J. D., Chan, M. N., Seinfeld, J. H., Edgerton, E. S., Su, Y., and Prather, K.

542   A.: Measurements of isoprene-derived organosulfates in ambient aerosols by aerosol time-of-flight mass spectrometry-part 2:

543   temporal variability and formation mechanisms, Environ. Sci. Technol., 45, 8648-8655, 10.1021/es2011836, 2011.

544   Hawkins, L. N., Russell, L. M., Covert, D. S., Quinn, P. K., and Bates, T. S.: Carboxylic acids, sulfates, and organosulfates in

545   processed continental organic aerosol over the southeast Pacific Ocean during VOCALS-REx 2008, J. Geophys. Res.,

546   [Atmos.], 115, D13201, 10.1029/2009jd013276, 2010.

547   He, Q. F., Ding, X., Wang, X. M., Yu, J. Z., Fu, X. X., Liu, T. Y., Zhang, Z., Xue, J., Chen, D. H., Zhong, L. J., and Donahue,

548   N. M.: Organosulfates from pinene and isoprene over the Pearl River Delta, South China: seasonal variation and implication

549   in formation mechanisms, Environ. Sci. Technol., 48, 9236-9245, 10.1021/es501299v, 2014.

550   He, S., Chen, Z., and Zhang, X.: Photochemical reactions of methyl and ethyl nitrate: a dual role for alkyl nitrates in the

551   nitrogen cycle, Environ. Chem., 8, 529, 10.1071/en10004, 2011.

552   Hennigan, C. J., Izumi, J., Sullivan, A. P., Weber, R. J., and Nenes, A.: A critical evaluation of proxy methods used to

553   estimate the acidity of atmospheric particles, Atmos. Chem. Phys., 15, 2775-2790, 10.5194/acp-15-2775-2015, 2015.

554   Hettiyadura, A. P. S., Stone, E. A., Kundu, S., Baker, Z., Geddes, E., Richards, K., and Humphry, T.: Determination of

555   atmospheric organosulfates using HILIC chromatography with MS detection, Atmos. Meas. Tech., 8, 2347-2358,

556   10.5194/amt-8-2347-2015, 2015.

557   Hettiyadura, A. P. S., Jayarathne, T., Baumann, K., Goldstein, A. H., de Gouw, J. A., Koss, A., Keutsch, F. N., Skog, K., and

558   Stone, E. A.: Qualitative and quantitative analysis of atmospheric organosulfates in Centreville, Alabama, Atmos. Chem.

559   Phys., 17, 1343-1359, 10.5194/acp-17-1343-2017, 2017.

560   Hu, K. S., Darer, A. I., and Elrod, M. J.: Thermodynamics and kinetics of the hydrolysis of atmospherically relevant

561   organonitrates and organosulfates, Atmos. Chem. Phys., 11, 8307-8320, 10.5194/acp-11-8307-2011, 2011.

562   Iinuma, Y., Muller, C., Berndt, T., Boge, O., Claeys, M., and Herrmann, H.: Evidence for the existence of organosulfates

563   from β-pinene ozonolysis in ambient secondary organic aerosol, Environ. Sci. Technol., 41, 6678-6683, 10.1021/es070938t,
564   2007.

565   Jimenez, J. L., Canagaratna, M. R., Donahue, N. M., Prevot, A. S., Zhang, Q., Kroll, J. H., DeCarlo, P. F., Allan, J. D., Coe,
566   H., Ng, N. L., Aiken, A. C., Docherty, K. S., Ulbrich, I. M., Grieshop, A. P., Robinson, A. L., Duplissy, J., Smith, J. D.,
567   Wilson, K. R., Lanz, V. A., Hueglin, C., Sun, Y. L., Tian, J., Laaksonen, A., Raatikainen, T., Rautiainen, J., Vaattovaara, P.,
568   Ehn, M., Kulmala, M., Tomlinson, J. M., Collins, D. R., Cubison, M. J., Dunlea, E. J., Huffman, J. A., Onasch, T. B., Alfarra,
569   M. R., Williams, P. I., Bower, K., Kondo, Y., Schneider, J., Drewnick, F., Borrmann, S., Weimer, S., Demerjian, K., Salcedo,
570   D., Cottrell, L., Griffin, R., Takami, A., Miyoshi, T., Hatakeyama, S., Shimono, A., Sun, J. Y., Zhang, Y. M., Dzepina, K.,
571   Kimmel, J. R., Sueper, D., Jayne, J. T., Herndon, S. C., Trimborn, A. M., Williams, L. R., Wood, E. C., Middlebrook, A. M.,
572   Kolb, C. E., Baltensperger, U., and Worsnop, D. R.: Evolution of organic aerosols in the atmosphere, Science, 326,
573   1525-1529, 10.1126/science.1180353, 2009.

574   Kiehl, J. T.: Twentieth century climate model response and climate sensitivity, Geophys. Res. Lett., 34,
575   10.1029/2007gl031383, 2007.

576   Kroll, J. H., and Seinfeld, J. H.: Chemistry of secondary organic aerosol: Formation and evolution of low-volatility organics
577   in the atmosphere, Atmos. Environ., 42, 3593-3624, 10.1016/j.atmosenv.2008.01.003, 2008.

578   Lal, V., Khalizov, A. F., Lin, Y., Galvan, M. D., Connell, B. T., and Zhang, R.: Heterogeneous reactions of epoxides in acidic
579   media, The journal of physical chemistry. A, 116, 6078-6090, 10.1021/jp2112704, 2012.

580   Lee, B. H., Mohr, C., Lopez-Hilfiker, F. D., Lutz, A., Hallquist, M., Lee, L., Romer, P., Cohen, R. C., Iyer, S., Kurten, T., Hu,
581   W., Day, D. A., Campuzano-Jost, P., Jimenez, J. L., Xu, L., Ng, N. L., Guo, H., Weber, R. J., Wild, R. J., Brown, S. S., Koss,
582   A., de Gouw, J., Olson, K., Goldstein, A. H., Seco, R., Kim, S., McAvey, K., Shepson, P. B., Starn, T., Baumann, K.,
583   Edgerton, E. S., Liu, J., Shilling, J. E., Miller, D. O., Brune, W., Schobesberger, S., D'Ambro, E. L., and Thornton, J. A.:
584   Highly functionalized organic nitrates in the southeast United States: Contribution to secondary organic aerosol and reactive
585   nitrogen budgets, Proc. Natl. Acad. Sci. USA, 113, 1516-1521, 10.1073/pnas.1508108113, 2016.

586   Li, W., Sun, J., Xu, L., Shi, Z., Riemer, N., Sun, Y., Fu, P., Zhang, J., Lin, Y., Wang, X., Shao, L., Chen, J., Zhang, X., Wang,
587   Z., and Wang, W.: A conceptual framework for mixing structures in individual aerosol particles, J. Geophys. Res., [Atmos.],
588   121, 13,784-713,798, 10.1002/2016jd025252, 2016.

589   Liao, J., Froyd, K. D., Murphy, D. M., Keutsch, F. N., Yu, G., Wennberg, P. O., St Clair, J. M., Crounse, J. D., Wisthaler, A.,
590   Mikoviny, T., Jimenez, J. L., Campuzano-Jost, P., Day, D. A., Hu, W., Ryerson, T. B., Pollack, I. B., Peischl, J., Anderson, B.
591   E., Ziemba, L. D., Blake, D. R., Meinardi, S., and Diskin, G.: Airborne measurements of organosulfates over the continental
592   U.S, J. Geophys. Res., [Atmos.], 120, 2990-3005, 10.1002/2014JD022378, 2015.

593   Liggio, J., and Li, S.-M.: Organosulfate formation during the uptake of pinonaldehyde on acidic sulfate aerosols, Geophys.
594   Res. Lett., 33, 10.1029/2006gl026079, 2006.

595   Lin, P., Huang, X. F., He, L. Y., and Yu, J. Z.: Abundance and size distribution of HULIS in ambient aerosols at a rural site in
596   South China, J. Aerosol Sci., 41, 74-87, 10.1016/j.jaerosci.2009.09.001, 2010.

597   Lin, P., Yu, J. Z., Engling, G., and Kalberer, M.: Organosulfates in humic-like substance fraction isolated from aerosols at
598   seven locations in East Asia: a study by ultra-high-resolution mass spectrometry, Environ. Sci. Technol., 46, 13118-13127,
599   10.1021/es303570v, 2012.

Atmospheric
Chemistry
and Physics
Discussions

600   Lin, Y. H., Knipping, E. M., Edgerton, E. S., Shaw, S. L., and Surratt, J. D.: Investigating the influences of SO_2 and NH_3
601   levels on isoprene-derived secondary organic aerosol formation using conditional sampling approaches, Atmos. Chem. Phys.,
602   13, 8457-8470, 10.5194/acp-13-8457-2013, 2013a.

603   Lin, Y. H., Zhang, H., Pye, H. O., Zhang, Z., Marth, W. J., Park, S., Arashiro, M., Cui, T., Budisulistiorini, S. H., Sexton, K.
604   G., Vizuete, W., Xie, Y., Luecken, D. J., Piletic, I. R., Edney, E. O., Bartolotti, L. J., Gold, A., and Surratt, J. D.: Epoxide as a
605   precursor to secondary organic aerosol formation from isoprene photooxidation in the presence of nitrogen oxides, Proc. Natl.
606   Acad. Sci. USA, 110, 6718-6723, 10.1073/pnas.1221150110, 2013b.

607   Liu, M., Song, Y., Zhou, T., Xu, Z., Yan, C., Zheng, M., Wu, Z., Hu, M., Wu, Y., and Zhu, T.: Fine particle pH during severe
608   haze episodes in northern China, Geophys. Res. Lett., 44, 5213-5221, 10.1002/2017gl073210, 2017.

609   Ma, Y., Xu, X. K., Song, W. H., Geng, F. H., and Wang, L.: Seasonal and diurnal variations of particulate organosulfates in
610   urban Shanghai, China, Atmos. Environ., 85, 152-160, 10.1016/j.atmosenv.2013.12.017, 2014.

611   McNeill, V. F., Woo, J. L., Kim, D. D., Schwier, A. N., Wannell, N. J., Sumner, A. J., and Barakat, J. M.: Aqueous-phase
612   secondary organic aerosol and organosulfate formation in atmospheric aerosols: a modeling study, Environ. Sci. Technol., 46,
613   8075-8081, 10.1021/es3002986, 2012.

614   McNeill, V. F.: Aqueous organic chemistry in the atmosphere: sources and chemical processing of organic aerosols, Environ.
615   Sci. Technol., 49, 1237-1244, 10.1021/es5043707, 2015.

616   Meade, L. E., Riva, M., Blomberg, M. Z., Brock, A. K., Qualters, E. M., Siejack, R. A., Ramakrishnan, K., Surratt, J. D., and
617   Kautzman, K. E.: Seasonal variations of fine particulate organosulfates derived from biogenic and anthropogenic
618   hydrocarbons in the mid-Atlantic United States, Atmos. Environ., 145, 405-414, 10.1016/j.atmosenv.2016.09.028, 2016.

619   Minerath, E. C., Casale, M. T., and Elrod, M. J.: Kinetics Feasibility Study of Alcohol Sulfate Esterification Reactions in
620   Tropospheric Aerosols, Environ. Sci. Technol., 42, 4410-4415, 10.1021/es8004333, 2008.

621   Minerath, E. C., and Elrod, M. J.: Assessing the potential for diol and hydroxy sulfate ester formation from the reaction of
622   epoxides in tropospheric aerosols, Environ. Sci. Technol., 43, 1386-1392, 10.1021/es8029076, 2009.

623   Nguyen, T. B., Bates, K. H., Crounse, J. D., Schwantes, R. H., Zhang, X., Kjaergaard, H. G., Surratt, J. D., Lin, P., Laskin, A.,
624   Seinfeld, J. H., and Wennberg, P. O.: Mechanism of the hydroxyl radical oxidation of methacryloyl peroxynitrate (MPAN)
625   and its pathway toward secondary organic aerosol formation in the atmosphere, Phys. Chem. Chem. Phys., 17, 17914-17926,
626   10.1039/c5cp02001h, 2015.

627   Nozière, B., Ekström, S., Alsberg, T., and Holmström, S.: Radical-initiated formation of organosulfates and surfactants in
628   atmospheric aerosols, Geophys. Res. Lett., 37, 10.1029/2009gl041683, 2010.

629   Olson, C. N., Galloway, M. M., Yu, G., Hedman, C. J., Lockett, M. R., Yoon, T., Stone, E. A., Smith, L. M., and Keutsch, F.
630   N.: Hydroxycarboxylic acid-derived organosulfates: synthesis, stability, and quantification in ambient aerosol, Environ. Sci.
631   Technol., 45, 6468-6474, 10.1021/es201039p, 2011.

632   Paulot, F., Crounse, J. D., Kjaergaard, H. G., Kurten, A., St Clair, J. M., Seinfeld, J. H., and Wennberg, P. O.: Unexpected
633   epoxide formation in the gas-phase photooxidation of isoprene, Science, 325, 730-733, 10.1126/science.1172910, 2009.

634   Rattanavaraha, W., Chu, K., Budisulistiorini, S. H., Riva, M., Lin, Y.-H., Edgerton, E. S., Baumann, K., Shaw, S. L., Guo, H.,
635   King, L., Weber, R. J., Neff, M. E., Stone, E. A., Offenberg, J. H., Zhang, Z., Gold, A., and Surratt, J. D.: Assessing the
636   impact of anthropogenic pollution on isoprene-derived secondary organic aerosol formation in $PM_{2.5}$ collected from the

637   Birmingham, Alabama, ground site during the 2013 Southern Oxidant and Aerosol Study, Atmos. Chem. Phys., 16,
638   4897-4914, 10.5194/acp-16-4897-2016, 2016.

639   Renbaum-Wolff, L., Grayson, J. W., Bateman, A. P., Kuwata, M., Sellier, M., Murray, B. J., Shilling, J. E., Martin, S. T., and
640   Bertram, A. K.: Viscosity of α-pinene secondary organic material and implications for particle growth and reactivity, Proc.
641   Natl. Acad. Sci. USA, 110, 8014-8019, 10.1073/pnas.1219548110, 2013.

642   Riva, M., Tomaz, S., Cui, T., Lin, Y. H., Perraudin, E., Gold, A., Stone, E. A., Villenave, E., and Surratt, J. D.: Evidence for
643   an unrecognized secondary anthropogenic source of organosulfates and sulfonates: gas-phase oxidation of polycyclic
644   aromatic hydrocarbons in the presence of sulfate aerosol, Environ. Sci. Technol., 49, 6654-6664, 10.1021/acs.est.5b00836,
645   2015.

646   Riva, M., Budisulistiorini, S. H., Zhang, Z., Gold, A., and Surratt, J. D.: Chemical characterization of secondary organic
647   aerosol constituents from isoprene ozonolysis in the presence of acidic aerosol, Atmos. Environ., 130, 5-13,
648   10.1016/j.atmosenv.2015.06.027, 2016a.

649   Riva, M., Da Silva Barbosa, T., Lin, Y.-H., Stone, E. A., Gold, A., and Surratt, J. D.: Chemical characterization of
650   organosulfates in secondary organic aerosol derived from the photooxidation of alkanes, Atmos. Chem. Phys., 16,
651   11001-11018, 10.5194/acp-16-11001-2016, 2016b.

652   Schindelka, J., Iinuma, Y., Hoffmann, D., and Herrmann, H.: Sulfate radical-initiated formation of isoprene-derived
653   organosulfates in atmospheric aerosols, Faraday Discussions, 165, 237, 10.1039/c3fd00042g, 2013.

654   Shalamzari, M. S., Kahnt, A., Vermeylen, R., Kleindienst, T. E., Lewandowski, M., Cuyckens, F., Maenhaut, W., and Claeys,
655   M.: Characterization of polar organosulfates in secondary organic aerosol from the green leaf volatile 3-Z-hexenal, Environ.
656   Sci. Technol., 48, 12671-12678, 10.1021/es503226b, 2014.

657   Shalamzari, M. S., Vermeylen, R., Blockhuys, F., Kleindienst, T. E., Lewandowski, M., Szmigielski, R., Rudzinski, K. J.,
658   Spólnik, G., Danikiewicz, W., Maenhaut, W., and Claeys, M.: Characterization of polar organosulfates in secondary organic
659   aerosol from the unsaturated aldehydes 2-E-pentenal, 2-E-hexenal, and 3-Z-hexenal, Atmos. Chem. Phys., 16, 7135-7148,
660   10.5194/acp-16-7135-2016, 2016.

661   Shiraiwa, M., Ammann, M., Koop, T., and Poschl, U.: Gas uptake and chemical aging of semisolid organic aerosol particles,
662   Proc. Natl. Acad. Sci. USA, 108, 11003-11008, 10.1073/pnas.1103045108, 2011.

663   Shrivastava, M., Cappa, C. D., Fan, J., Goldstein, A. H., Guenther, A. B., Jimenez, J. L., Kuang, C., Laskin, A., Martin, S. T.,
664   Ng, N. L., Petaja, T., Pierce, J. R., Rasch, P. J., Roldin, P., Seinfeld, J. H., Shilling, J., Smith, J. N., Thornton, J. A., Volkamer,
665   R., Wang, J., Worsnop, D. R., Zaveri, R. A., Zelenyuk, A., and Zhang, Q.: Recent advances in understanding secondary
666   organic aerosol: Implications for global climate forcing, Rev. Geophys., 55, 509-559, 10.1002/2016rg000540, 2017.

667   Staudt, S., Kundu, S., Lehmler, H. J., He, X., Cui, T., Lin, Y. H., Kristensen, K., Glasius, M., Zhang, X., Weber, R. J., Surratt,
668   J. D., and Stone, E. A.: Aromatic organosulfates in atmospheric aerosols: synthesis, characterization, and abundance, Atmos
669   Environ (1994), 94, 366-373, 10.1016/j.atmosenv.2014.05.049, 2014.

670   Stone, E. A., Yang, L., Yu, L. E., and Rupakheti, M.: Characterization of organosulfates in atmospheric aerosols at Four
671   Asian locations, Atmos. Environ., 47, 323-329, 10.1016/j.atmosenv.2011.10.058, 2012.

672   Suarez-Bertoa, R., Picquet-Varrault, B., Tamas, W., Pangui, E., and Doussin, J. F.: Atmospheric fate of a series of carbonyl
673   nitrates: photolysis frequencies and OH-oxidation rate constants, Environ. Sci. Technol., 46, 12502-12509,

674   10.1021/es302613x, 2012.

675   Surratt, J. D., Kroll, J. H., Kleindienst, T. E., Edney, E. O., Claeys, M., Sorooshian, A., Ng, N. L., Offenberg, J. H.,

676   Lewandowski, M., Jaoui, M., Flagan, R. C., and Seinfeld, J. H.: Evidence for Organosulfates in Secondary Organic Aerosol,

677   Environ. Sci. Technol., 41, 517-527, 10.1021/es062081q, 2007.

678   Surratt, J. D., Gomez-Gonzalez, Y., Chan, A. W., Vermeylen, R., Shahgholi, M., Kleindienst, T. E., Edney, E. O., Offenberg,

679   J. H., Lewandowski, M., Jaoui, M., Maenhaut, W., Claeys, M., Flagan, R. C., and Seinfeld, J. H.: Organosulfate formation in

680   biogenic secondary organic aerosol, J. Phys. Chem. A, 112, 8345-8378, 10.1021/jp802310p, 2008.

681   Surratt, J. D., Chan, A. W., Eddingsaas, N. C., Chan, M., Loza, C. L., Kwan, A. J., Hersey, S. P., Flagan, R. C., Wennberg, P.

682   O., and Seinfeld, J. H.: Reactive intermediates revealed in secondary organic aerosol formation from isoprene, Proc. Natl.

683   Acad. Sci. USA, 107, 6640-6645, 10.1073/pnas.0911114107, 2010.

684   Tang, R., Wu, Z., Li, X., Wang, Y., Shang, D., Xiao, Y., Li, M., Zeng, L., Wu, Z., Hallquist, M., Hu, M., and Guo, S.: Primary

685   and secondary organic aerosols in 2016 summer of Beijing, Atmos. Chem. Phys., 1-35, 10.5194/acp-2017-867, 2017.

686   Tao, S., Lu, X., Levac, N., Bateman, A. P., Nguyen, T. B., Bones, D. L., Nizkorodov, S. A., Laskin, J., Laskin, A., and Yang,

687   X.: Molecular characterization of organosulfates in organic aerosols from Shanghai and Los Angeles urban areas by

688   nanospray-desorption electrospray ionization high-resolution mass spectrometry, Environ. Sci. Technol., 48, 10993-11001,

689   10.1021/es5024674, 2014.

690   Tolocka, M. P., and Turpin, B.: Contribution of organosulfur compounds to organic aerosol mass, Environ. Sci. Technol., 46,

691   7978-7983, 10.1021/es300651v, 2012.

692   Turpin, B. J., and Lim, H.-J.: Species Contributions to PM2.5 Mass Concentrations: Revisiting Common Assumptions for

693   Estimating Organic Mass, Aerosol Sci. Tech., 35, 602-610, 10.1080/027868201119445, 2001.

694   Vaden, T. D., Imre, D., Beranek, J., Shrivastava, M., and Zelenyuk, A.: Evaporation kinetics and phase of laboratory and

695   ambient secondary organic aerosol, Proc. Natl. Acad. Sci. USA, 108, 2190-2195, 10.1073/pnas.1013391108, 2011.

696   Wang, H., Chen, J., and Lu, K.: Development of a portable cavity-enhanced absorption spectrometer for the measurement of

697   ambient NO_3 and N_2O_5: experimental setup, lab characterizations, and field applications in a polluted urban environment,

698   Atmos. Meas. Tech., 10, 1465-1479, 10.5194/amt-10-1465-2017, 2017a.

699   Wang, H., Lu, K., Chen, X., Zhu, Q., Chen, Q., Guo, S., Jiang, M., Li, X., Shang, D., Tan, Z., Wu, Y., Wu, Z., Zou, Q., Zheng,

700   Y., Zeng, L., Zhu, T., Hu, M., and Zhang, Y.: High N_2O_5 Concentrations Observed in Urban Beijing: Implications of a Large

701   Nitrate Formation Pathway, Environmental Science & Technology Letters, 4, 416-420, 10.1021/acs.estlett.7b00341, 2017b.

702   Wang, H., Lu, K., Guo, S., Wu, Z., Shang, D., Tan, Z., Wang, Y., Le Breton, M., Zhu, W., Lou, S., Tang, M., Wu, Y., Zheng,

703   J., Zeng, L., Hallquist, M., Hu, M., and Zhang, Y.: Efficient N_2O_5 Uptake and NO_3 Oxidation in the Outflow of Urban

704   Beijing, Atmos. Chem. Phys. Disc., 1-27, 10.5194/acp-2018-88, 2018.

705   Wang, X. K., Rossignol, S., Ma, Y., Yao, L., Wang, M. Y., Chen, J. M., George, C., and Wang, L.: Molecular characterization

706   of atmospheric particulate organosulfates in three megacities at the middle and lower reaches of the Yangtze River, Atmos.

707   Chem. Phys., 16, 2285-2298, 10.5194/acp-16-2285-2016, 2016.

708   Wang, Y., Hu, M., Lin, P., Guo, Q., Wu, Z., Li, M., Zeng, L., Song, Y., Zeng, L., Wu, Y., Guo, S., Huang, X., and He, L.:

709   Molecular Characterization of Nitrogen-Containing Organic Compounds in Humic-like Substances Emitted from Straw

710   Residue Burning, Environ. Sci. Technol., 51, 5951-5961, 10.1021/acs.est.7b00248, 2017c.

711 Wang, Y., Ren, J., Huang, X. H. H., Tong, R., and Yu, J. Z.: Synthesis of Four Monoterpene-Derived Organosulfates and
712 Their Quantification in Atmospheric Aerosol Samples, Environ. Sci. Technol., 51, 6791-6801, 10.1021/acs.est.7b01179,
713 2017d.
714 Weber, R. J., Guo, H., Russell, A. G., and Nenes, A.: High aerosol acidity despite declining atmospheric sulfate
715 concentrations over the past 15 years, Nature Geosci., 9, 282-285, 10.1038/ngeo2665, 2016.
716 Worton, D. R., Surratt, J. D., Lafranchi, B. W., Chan, A. W., Zhao, Y., Weber, R. J., Park, J. H., Gilman, J. B., de Gouw, J.,
717 Park, C., Schade, G., Beaver, M., Clair, J. M., Crounse, J., Wennberg, P., Wolfe, G. M., Harrold, S., Thornton, J. A., Farmer,
718 D. K., Docherty, K. S., Cubison, M. J., Jimenez, J. L., Frossard, A. A., Russell, L. M., Kristensen, K., Glasius, M., Mao, J.,
719 Ren, X., Brune, W., Browne, E. C., Pusede, S. E., Cohen, R. C., Seinfeld, J. H., and Goldstein, A. H.: Observational insights
720 into aerosol formation from isoprene, Environ. Sci. Technol., 47, 11403-11413, 10.1021/es4011064, 2013.
721 Wu, Z., Wang, Y., Tan, T., Zhu, Y., Li, M., Shang, D., Wang, H., Lu, K., Guo, S., Zeng, L., and Zhang, Y.: Aerosol Liquid
722 Water Driven by Anthropogenic Inorganic Salts: Implying Its Key Role in Haze Formation over the North China Plain,
723 Environmental Science & Technology Letters, 10.1021/acs.estlett.8b00021, 2018.
724 Xu L., Guo H., Boyd C. M., Klein M., Bougiatioti A., Cerully K., Hite J., Wertz G., Kreisberg N., Knote C., Olson K., Koss
725 A., Goldstein A., Hering S., Gouw J., Baumann K., Lee S., Nenes A., Weber R., and Ng, N. L: Effects of anthropogenic
726 emissions on aerosol formation from isoprene and monoterpenes in the southeastern United States, Proc. Natl. Acad. Sci.
727 USA, 112, E4506-4507, 10.1073/pnas.1417609112, 2015.
728 Xue, J., Griffith, S. M., Yu, X., Lau, A. K. H., and Yu, J. Z.: Effect of nitrate and sulfate relative abundance in $PM_{2.5}$ on liquid
729 water content explored through half-hourly observations of inorganic soluble aerosols at a polluted receptor site, Atmos.
730 Environ., 99, 24-31, 10.1016/j.atmosenv.2014.09.049, 2014.
731 Zhang, H., Worton, D. R., Lewandowski, M., Ortega, J., Rubitschun, C. L., Park, J. H., Kristensen, K., Campuzano-Jost, P.,
732 Day, D. A., Jimenez, J. L., Jaoui, M., Offenberg, J. H., Kleindienst, T. E., Gilman, J., Kuster, W. C., de Gouw, J., Park, C.,
733 Schade, G. W., Frossard, A. A., Russell, L., Kaser, L., Jud, W., Hansel, A., Cappellin, L., Karl, T., Glasius, M., Guenther, A.,
734 Goldstein, A. H., Seinfeld, J. H., Gold, A., Kamens, R. M., and Surratt, J. D.: Organosulfates as tracers for secondary organic
735 aerosol (SOA) formation from 2-methyl-3-buten-2-ol (MBO) in the atmosphere, Environ. Sci. Technol., 46, 9437-9446,
736 10.1021/es301648z, 2012.
737 Zhang, Y., Chen, Y., Lambe, A. T., Olson, N. E., Lei, Z., Craig, R. L., Zhang, Z., Gold, A., Onasch, T. B., Jayne, J. T.,
738 Worsnop, D. R., Gaston, C. J., Thornton, J. A., Vizuete, W., Ault, A. P., and Surratt, J. D.: Effect of the Aerosol-Phase State
739 on Secondary Organic Aerosol Formation from the Reactive Uptake of Isoprene-Derived Epoxydiols (IEPOX),
740 Environmental Science & Technology Letters, 5, 167-174, 10.1021/acs.estlett.8b00044, 2018.
741 Zheng, J., Hu, M., Du, Z. F., Shang, D. J., Gong, Z. H., Qin, Y. H., Fang, J. Y., Gu, F. T., Li, M. R., Peng, J. F., Li, J., Zhang,
742 Y. Q., Huang, X. F., He, L. Y., Wu, Y. S., and Guo, S.: Influence of biomass burning from South Asia at a high-altitude
743 mountain receptor site in China, Atmos. Chem. Phys., 17, 6853-6864, 10.5194/acp-17-6853-2017, 2017.

744
745
746
747

748

Figures

750

751
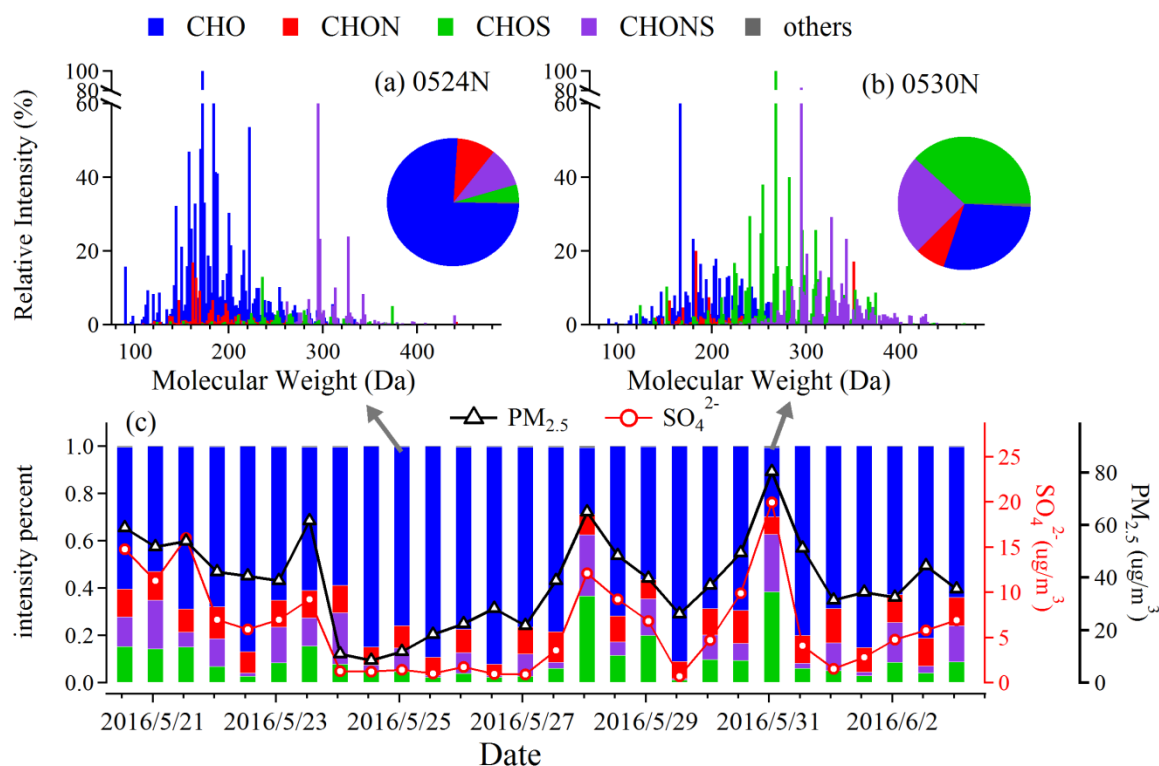
Figure 1 The intensity distribution of different compound categories (CHO, CHON, CHOS and CHONS) (a) on a clean day

and (b) on a polluted day. (c) Temporal variation of $PM_{2.5}$, SO_4^{2-} and intensity percentages of different compound categories.

The highly water-soluble OS species (e.g. isoprene OSs) with lower MW are absent in these figures and details were
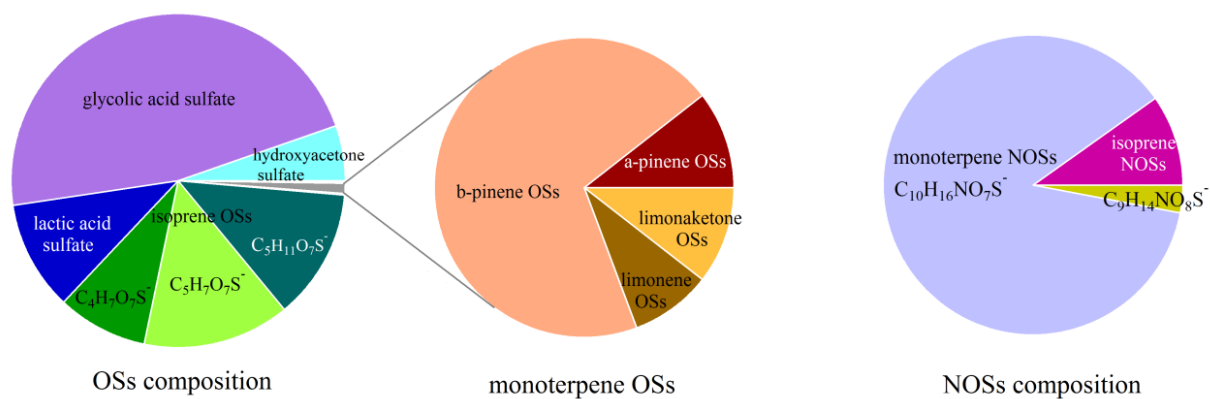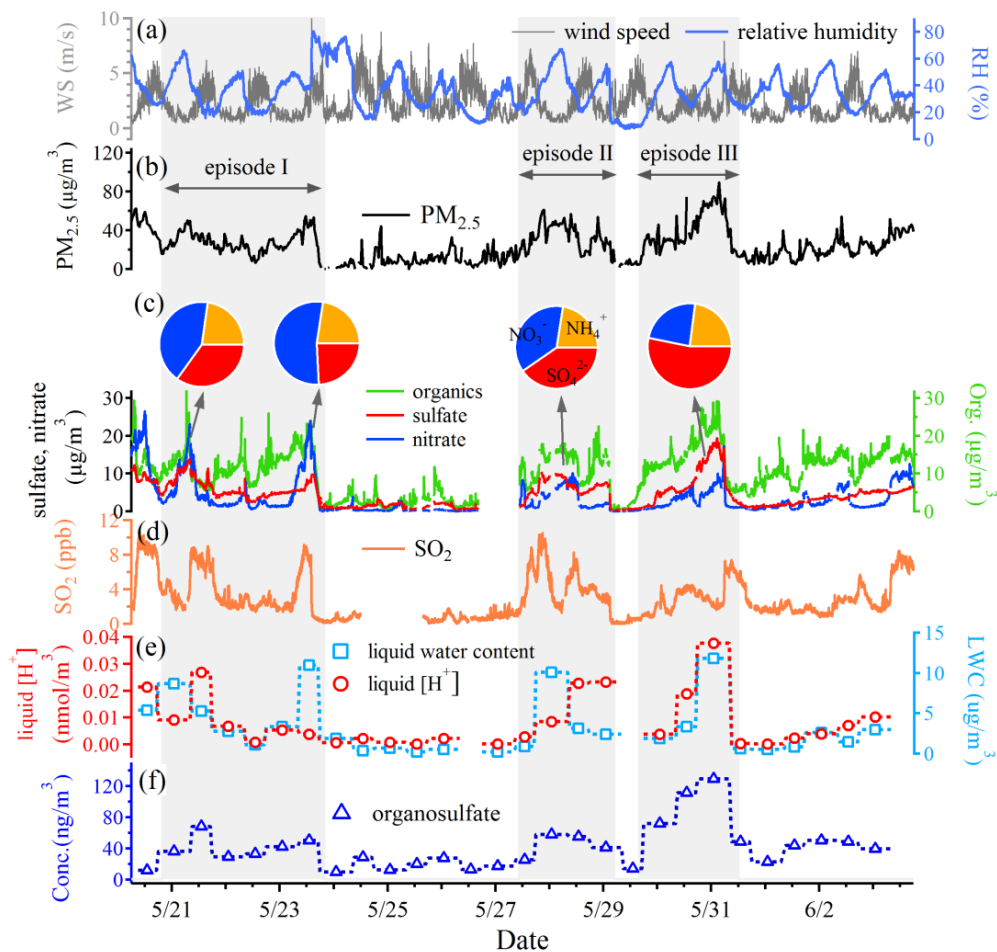
described in the text.

756

757

758

759

760

Figure 2 The relative contribution of different OS and NOS species.

763

764

765

Figure 3 Time series of (a) wind speed (WS) and relative humidity (RH), (b) $PM_{2.5}$, (c) mass concentrations of organics, sulfate, nitrate and composition of secondary inorganic aerosols during pollution episodes (d) SO_2, (e) liquid water content (LWC) and aqueous phase $[H^+]$, and (f) the total concentrations of OSs quantified by HPLC-MS. The pollution episodes were marked by gray shadow.

775

776
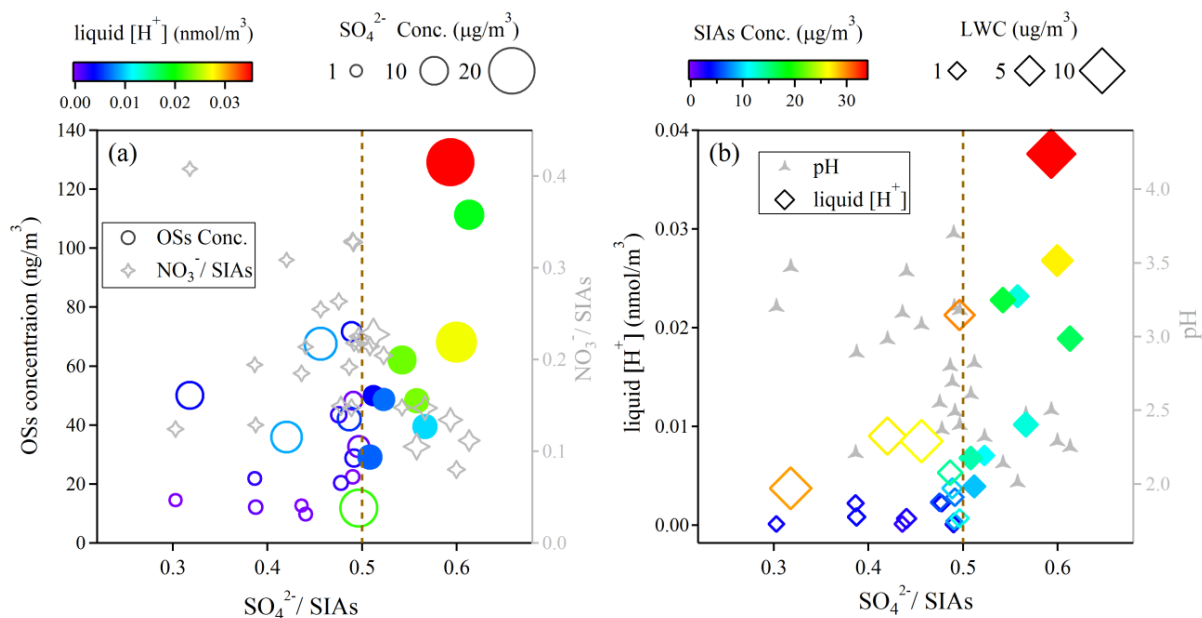
Figure 4 (a) The OS concentrations and NO_3^-/ SIAs mass ratios as a function of the SO_4^{2-}/ SIAs mass ratios. The circles are colored according to the liquid [H^+] concentration and the sizes of the circles are scaled to the SO_4^{2-} mass concentration. (b) The liquid [H^+] and aerosol pH as a function of the SO_4^{2-}/ SIAs mass ratios. The markers are colored according to the SIAs mass concentrations and the sizes of the markers are scaled to the liquid water content (LWC). The solid markers represent those among the range SO_4^{2-}/ SIAs > 0.5 and hollow markers represent those among the range SO_4^{2-}/ SIAs < 0.5 in figure (a) and (b).

784

785

786

787

Atmospheric
Chemistry
and Physics
Discussions

788
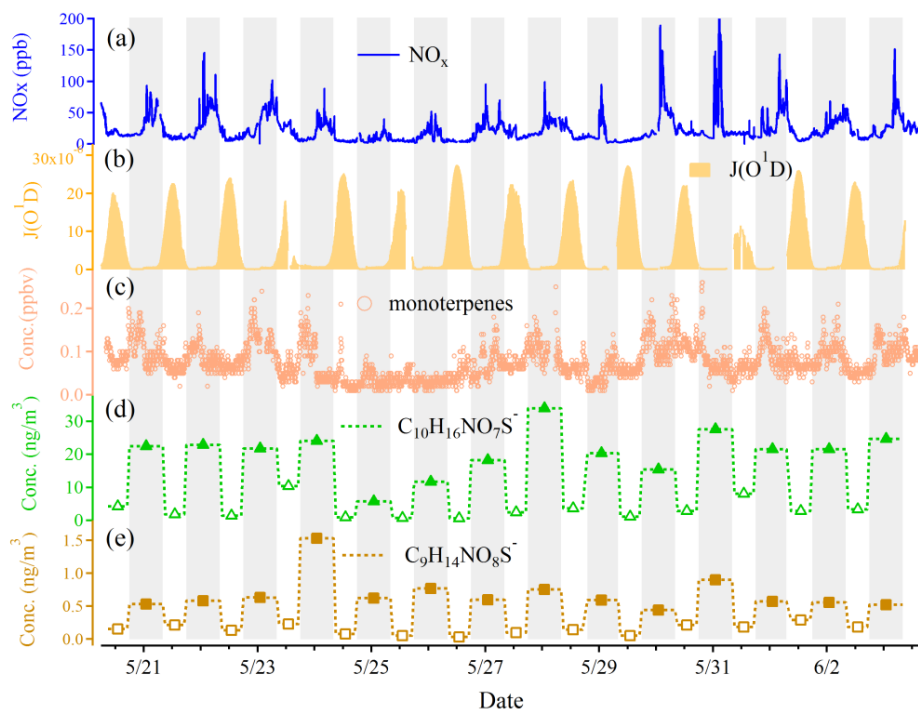
Figure 5 Time series of (a) NO_x, (b) $J(O^1D)$, (c) monoterpene, (d) monoterpene NOSs ($C_{10}H_{16}NO_7S^-$) and (e) limonaketone

NOSs ($C_9H_{14}NO_8S^-$). The gray background denotes the nighttime and white background denotes the daytime.

791

792

793

Atmospheric
Chemistry
and Physics
Discussions

794
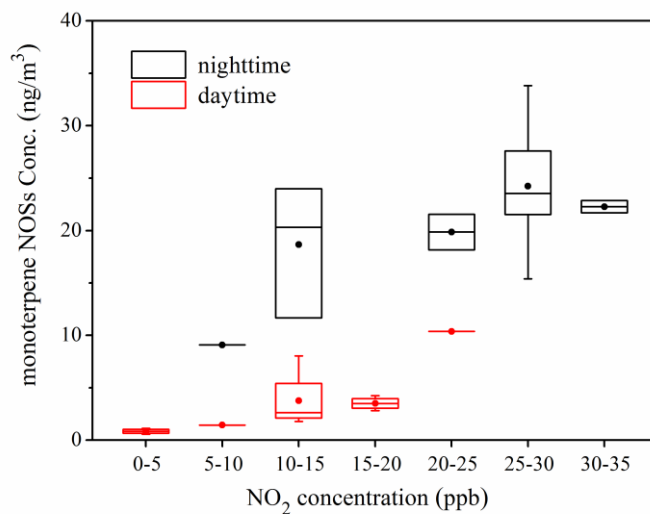
Figure 6 The concentrations of monoterpene NOSs ($C_{10}H_{16}NO_7S^-$) as a function of NO_2 concentration bins (ppb) during

daytime and nighttime. The closed circles represent the mean values and whiskers represent 25 and 75 percentiles.

797

798

Atmospheric
Chemistry
and Physics
Discussions

799
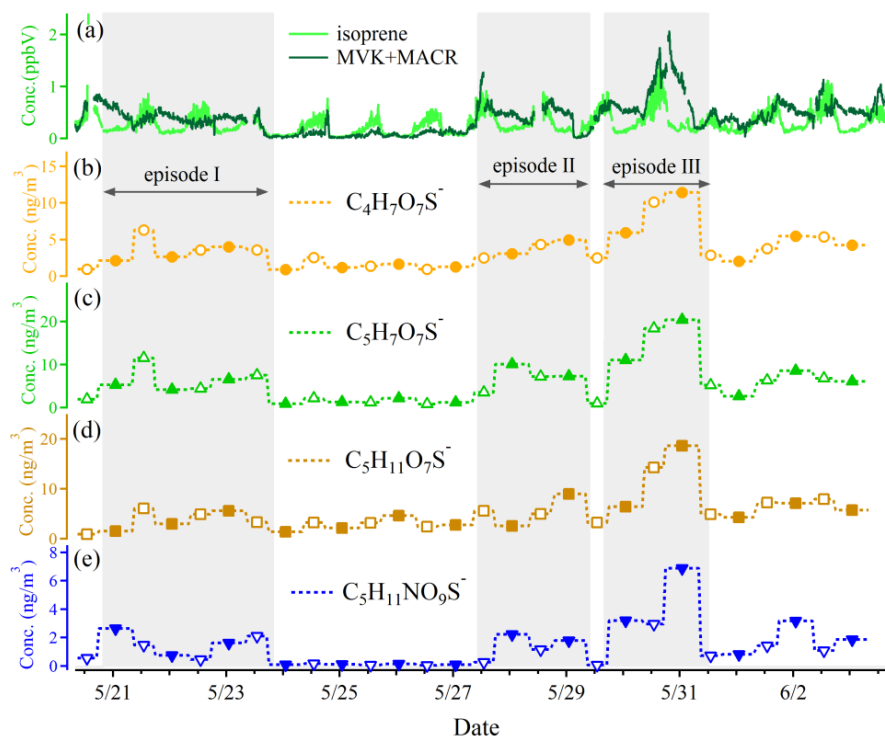
Figure 7 Time series of (a) isoprene and MVK+MACR, isoprene OSs (b) $C_4H_7O_7S^-$, (c) $C_5H_7O_7S^-$, (d) $C_5H_{11}O_7S^-$ and (e)

NOSs ($C_5H_{11}NO_9S^-$). The pollution episodes were marked by gray shadow. MVK and MACR are the abbreviations of

methyl vinyl ketone and methacrolein, respectively.

803

804
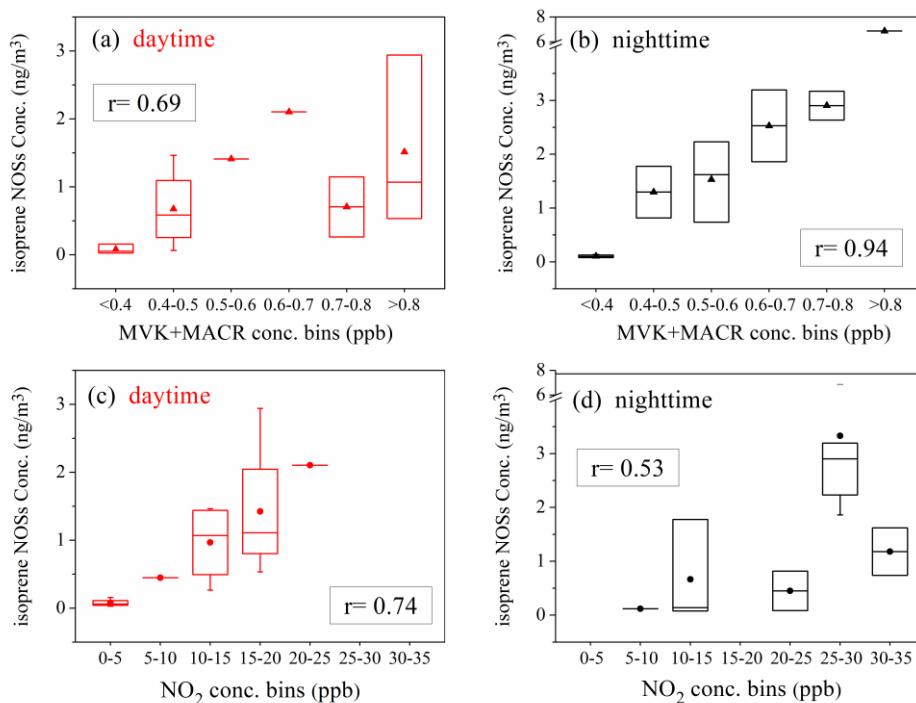
Figure 8 The isoprene NOSs ($C_5H_{11}NO_9S^-$) concentrations as a function of NO_2 or MVK+MACR concentration bins (ppb)

and the correlations between isoprene NOSs ($C_5H_{11}NO_9S^-$) and NO_2 or MVK+MACR. The closed markers in the box

represent the mean values and whiskers represent 25 and 75 percentiles in each concentration bin. The r value in each panel

represents the correlation coefficient between isoprene NOSs and NO_2 or MVK+MACR concentrations.

809

810

Atmospheric
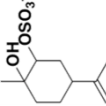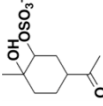Chemistry
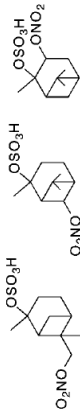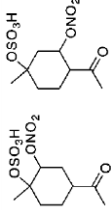and Physics
Discussions

Tables

Table 1 Organosulfates and nitrooxy-organosulfates quantified by HPLC-MS

common name	formula	[M-H]⁻	retention time (min)	standard	structure	concentration (ng/m³)	
						range	average (n=28)
Hydroxyacetone sulfate (HAS)	$C_3H_5O_5S^-$	152.99	1.7, 2.5	Glycolic acid sulfate	(Hettiyadura et al., 2015)	0.46-7.51	2.21
Glycolic acid sulfate (GAS)	$C_2H_3O_6S^-$	154.97	1.6, 2.3	Glycolic acid sulfate	(Olson et al., 2011)	3.86-58.16	19.50
Lactic acid sulfate (LAS)	$C_3H_5O_6S^-$	168.98	1.6, 2.6	Lactic acid sulfate	(Olson et al., 2011)	0.74-11.94	4.39
	$C_4H_7O_7S^-$	198.99	1.5, 2.9	Lactic acid sulfate	(Lin et al., 2013b; Surratt et al., 2007; Hettiyadura et al., 2015)	0.91-11.42	3.62
Isoprene OSs	$C_5H_7O_7S^-$	210.99	1.8, 2.9	Lactic acid sulfate	(Hettiyadura et al., 2015)	0.78-20.39	5.90
	$C_5H_{11}O_7S^-$	215.02	1.6, 2.0	Lactic acid sulfate	(He et al., 2014; Surratt et al., 2008)	0.87-18.68	5.25
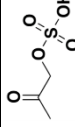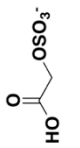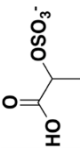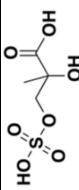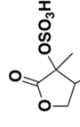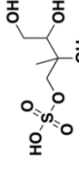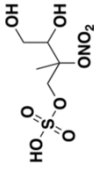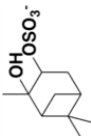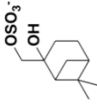
Name	Formula	m/z	t_R	Structure	Name	Range	Mean	Reference
Isoprene NOSs	$C_5H_{10}NO_9S^-$	260.01	4.9		Lactic acid sulfate	0.03-6.88	1.35	(Surratt et al., 2007)
α-pinene OSs	$C_{10}H_{17}O_5S^-$	249.08	22.7		α-pinene OS	0.01-0.51	0.06	(Wang et al., 2017d; Surratt et al., 2008)
β-pinene OSs	$C_{10}H_{17}O_5S^-$	249.08	22.4, 23.4		β-pinene OS	0.07-0.82	0.40	(Wang et al., 2017d; Surratt et al., 2008)
Limonene OSs	$C_{10}H_{17}O_5S^-$	249.08	21.8, 23.8		Limonene OS	0.01-0.13	0.05	(Wang et al., 2017d)
Limonaketone OSs	$C_9H_{15}O_6S^-$	251.06	14.0		Limonaketone OS	0.00-0.22	0.06	(Wang et al., 2017d)
Monoterpene NOSs	$C_{10}H_{16}NO_7S^-$	294.06	24.8, 26.6, 27.1		α-pinene OSs	0.56-33.84	11.99	(Surratt et al., 2008; He et al., 2014)
	$C_9H_{14}NO_8S^-$	296.04	21.1		Limonaketone OS	0.03-1.53	0.41	(Surratt et al., 2008)